Biological Function of *O*-linked Sugar Chain in Protein Quality Control

January 2008

Hiroto HIRAYAMA

Biological Function of *O*-linked Sugar Chain in Protein Quality Control

A Dissertation Submitted to
the Graduate School of Life and Environmental Sciences,
the University of Tsukuba
in Partial Fulfillment of the Requirements
for the Degree of Doctor of Philosophy in Science
(Doctoral Program in Functional Biosciences)

Hiroto HIRAYAMA

TABLE OF CONTENTS

ABBREVIATIONS

CHX	cycloheximide
CPY*	mutant carboxypeptidase Y
Dol	dolichol
Dol-P-Glc	dolicholphosphate-glucose
Dol-P-Man	dolicholphosphate-mannose
ER	endoplasmic reticulum
ERAD	endoplasmic reticulum-associated degradation
ERQC	endoplasmic reticulum quality control
Gas1*p	mutant form of Gas1p
GDP-Man	guanosinediphosphate-mannose
Glc	glucose
GlcNAc	*N*-acetyl glucosamine
GPI	glycosylphosphatidylinositol
HA	haemagglutinin
KHN	Kar2p signal sequence fused to simian virus 5 haemagglutinin neuraminidase
KHNt	HA-tagged yeast Kar2p signal sequence fusion to simian virus 5 haemagglutinin neuraminidase
LiAc	lithium acetate
Man	mannose

mutant pαF	mutant pro-α-factor
OD	optical density
Pmts	protein *O*-mannosyl transferase
PNGase F	peptide *N*-glycanase F
Δpro	pro-region-deleted derivative of *Rhizopus niveus* aspartic proteinase-I
sol-Gas1*p	non-GPI-anchored soluble version of Gas1*p
UDP-GlcNAc	uridinediphosphate-*N*-acetylglucosamine
UDP-Glc	uridinediphosphate-glucose

ABSTRACT

Protein glycosylation, which is the process of addition of sugar chains to proteins, is a principal post-translational modification in Eukaryotic cells. This process is a co-translational modification step in the newly synthesis of proteins and majority of proteins synthesized in the endoplasmic reticulum (ER) undergo glycosylation. Two types of glycosylation exist: *N*-linked glycosylation, which is bound to the amino nitrogen of asparagine (Asn) residues in the sequence of Asn-X-serine (Ser)/threonine (Thr) in the proteins, and *O*-linked glycosylation, which is bound to the hydroxy oxygen of Ser and Thr residues in the proteins. These two modifications served several physiological properties of newly synthesized proteins including protein stability, protein secretion, and protein folding. In particular, *N*-glycan plays an essential role in the folding process of newly synthesized proteins and endoplasmic reticulum-associate degradation (ERAD) of misfolded proteins.

In *Saccharomyces cerevisiae*, protein *O*-mannosylation, which is executed by protein *O*-mannosyltransferases (Pmts), is essential for a variety of biological processes as well as for conferring solubility to misfolded proteins. However, physiological function of *O*-mannosylation in the ER quality control (ERQC) systems is not well known. The work in this thesis focused on the physiological role of the *O*-mannosylation in the ERQC systems. First, I selected and analyzed a model misfolded protein HA-tagged Kar2p signal sequence fused to simian virus 5 haemagglutinin neuraminidase (KHNt), because it is reported that KHNt is a substrate for degradation

by the ERAD-L pathway, the substrate of which requires ER-to-Golgi transport for proteasome-dependent degradation (Vashist *et al.*, 2001). I found that in a *pmt1*Δ *pmt2*Δ double-mutant background, the degradation rate of KHNt is significantly decreased as compared to that of KHNt expressed in wild-type background cells. I further found that this defect of ERAD dependent degradation of KHNt in *pmt1*Δ *pmt2*Δ background is due to the severe aggregation of KHNt in the ER, notably, KHNt expressed in *pmt1*Δ *pmt2*Δ double-mutant cells forms detergent-insoluble aggregates. Taken together, my data suggested that KHNt *O*-mannosylation alleviates its aggregation and facilitates ER-to-Golgi transport of KHNt.

Second, I further investigated the molecular function of *O*-mannosylation in ERQC systems using another misfolded model protein Gas1*p. We previously generated Gas1*p, a misfolded ERAD substrate, and demonstrated that deacylation of the GPI anchor is important for the degradation of Gas1*p (Fujita *et al.*, 2006b). In the current study, I dissected the molecular role of *O*-mannosylation in degradation of misfolded proteins using Gas1*p. I found that Gas1*p is excessively *O*-mannosylated as compared to Gas1p. Pmt1p and Pmt2p, which are not responsible for *O*-mannosylation of correctly folded Gas1p, participate in *O*-mannosylation of Gas1*p. I further found that, in cells lacking both Pmt1p and Pmt2p function (*pmt1*Δ *pmt2*Δ), Gas1*p is transported to the vacuole via the endosomal sorting process, and degradation of Gas1*p shifts from a proteasome-dependent (ubiquitin/proteasome ERAD) to a vacuolar protease-dependent (post-ER degradation) pathway. These results support the idea that *O*-mannosylation of Gas1*p as catalyzed by Pmt1p and Pmt2p plays a crucial

role in degradation of Gas1*p through the ERAD pathway, which is dependent on proteasome degradation. This is the first report that a misfolded protein-specific *O*-mannosylation plays a role in not only alleviating their solubility but also facilitating ERAD-dependent degradation of misfolded proteins.

GENERAL INTRODUCTION

Proteins that are membrane bound or are destined for secretion are translated by ribosomes, associated with the membranes of the endoplasmic reticulum (ER), using mRNA as a template. Proteins are further modified post-translationally with several biochemical functional groups, such as, phosphate, ubiquitin, various lipids (e.g., GPI-anchor formation, myristoylation, and farnesylation), and carbohydrates, to change their structure and chemical nature. These modifications are collectively defined as a "post-translational modification", which is conserved in eukaryotic kingdom.

Glycosylation is one of the major post-translational modification

Protein modification with carbohydrates (glycosylation) is one of the most well known modifications in any eukaryotes. Two types of carbohydrate modification exist: *N*-linked glycosylation, which is bound to the amino nitrogen of asparagines (Asn) residues in the sequence of asparagine-X-serine/threonine (Asn-X-Ser/The; X can be any amino acid except proline) in the proteins, and *O*-linked glycosylation, which is bound to the hydroxyoxygen of Ser and Thr residues in the proteins. These two modifications serve several physiological functions of newly synthesized proteins including the protein activity, protein stability, protein secretion, protein folding, correct targeting, interaction between proteins, and cell–cell interaction in many living cells. It is presumed that about 50% of all eukaryotic proteins are modified by glycan (Kawasaki, 2003), and 90% of these glycosylated molecules are *N*-glycosylated. More

than 300 genes are involved in the glycan modification (glycogenes) including glycosyltransferases, glycosidases, and glycan binding proteins (lectins) in human genome (Taniguchi, 2003). There are many reports that the defects in glycogenes cause human diseases (e.g., congenital disorder of glycosylation (CDG), paroxysmal nocturnal hemoglobinuria (PNH), lysosomal storage diseases, and congenital muscular dystrophies (CMD)).

_N_-glycosylation in budding yeast, *Saccharomyces cerevisiae*

Most of the proteins produced in budding yeast *Saccharomyces cerevisiae*, a frequently used eukaryotic model organism, are glycosylated as well as in mammalian cells. For the formation of the glycan chains, including cell wall polysaccharide, more than 100 gene products are involved in yeast (Lehle *et al.*, 2006) (Figure 1). The biosynthetic pathway for *N*-glycan in the ER is conserved between yeast and mammal. The sequence of the reaction is shown in Figure 2.

In yeast, the genes and gene products responsible for the synthesis of the Dol-PP-oligosaccharide are largely known. In 1982, Huffacker and Robbins selected more than one dozen different mutants that had defects in the carbohydrate moiety using yeast genetics (Huffaker and Robbins, 1982). They applied a [^{3}H]-labeled mannose suicide method as a selection procedure. It is based on the principle that the desired mutants contain a reduced amount of [^{3}H]-labeled mannose and thus are exposed to a lower dose of lethal radioactivity. The mutants were designated as *alg* mutants, the corresponding

genes as *ALG* genes (Asparagine-Linked Glycosylation). In Figure 2, they are assigned to the respective reactions. The synthesis of the core oligosaccharide starts with the transfer of a GlcNAc-phosphate from uridinediphosphate-*N*-acetylglucosamine (UDP-GlcNAc) to dolicholphosphate giving rise to GlcNAc-PP-Dol. Then the transfer reactions of a second GlcNAc residue and five mannose residues are carried out by Alg family proteins in the cytosolic side of the ER, using the sugar nucleotides, UDP-GlcNAc and guanosinediphosphate-mannose (GDP-Man) as sugar donors (Burda and Aebi, 1999). Subsequently, the $Man_5GlcNAc_2$-PP-Dol was flipped to the luminal side (flip-flop) by the flippase Rft1p (Helenius *et al.*, 2002). There, the residual four mannoses and three glucoses were added according to a defined reaction sequence determined by the specificity of the individual glycosyltransferases. In the ER lumen, the lipid-activated sugars dolicholphosphate-mannose (Dol-P-Man) and dolicholphosphate-glucose (Dol-P-Glc) serve as sugar donors. With an artificial vesicle system, it was shown that after the synthesis of Dol-P-Man on the vesicle outer side, the mannose residue is translocated to the vesicle lumen (Haselbeck and Tanner, 1982). It remains uncertain, however, whether Dol-P-Man synthase, with the active site oriented to the cytosol, also catalyzes the transmembrane step or unidentified proteins participate in this step. With the help of the yeast-genome project completed in 1996, the genes for most reaction steps of the dolichol cycle have been identified through the complementation of the corresponding *alg* mutants.

The lipid-linked core oligosaccharide ($Glc_3Man_9GlcNAC_2$) is transferred, *en bloc*, to the polypeptide chain by the ER-resident oligosaccharyl transferase (OST)

complex (Kelleher and Gilmore, 2006). OST transfers a pre-assembled core oligosaccharide to the amino group of the Asn residue of the consensus sequence Asn-X-Ser/Thr, where X may be any amino acid except proline. The yeast OST has been identified by blue native electrophoresis to be a 240 kDa complex (Knauer and Lehle, 1999) and consists of at least eight subunits, Ost1p–Ost5p, Wbp1p, Swp1p, and Stt3p. Since *OST1*, *OST2*, *STT3*, *SWP1*, and *WBP1* are essential for growth, they are candidate for the active-site subunit of the OST. Several studies have shown that Stt3p is the central subunit involved in OST activity (Yan and Lennarz, 2002, Kelleher *et al.*, 2003, Yan and Lennarz, 2005). As soon as a protein acquires the oligosaccharide precursor ($Glc_3Man_9GlcNAc_2$), some trimming occurs in the ER. First, the terminal α-1,2-glucose residue is removed by α-glucosidase I. Then, the remaining two α-1,3-glucoses are cleaved off by α-glucosidase II. These steps occur similarly in yeast and mammalian cells. Then, a single mannose residue is cleaved off by α-1,2-mannosidase, the product of the *MNS1* gene. In yeast, the α-glucosidases I and II are encoded by *CWH41* and *ROT2*, respectively (reviewed by Herscovics, 1999).

The correctly folded glycoprotein precursors ($Man_8GlcNAc_2$) are transported to the Golgi apparatus and the glycans are further modified. In *S. cerevisiae*, *N*-glycan extends it further to make two general structures. One is a core-type structure, containing a few extra mannose residues, that is found on the intracellular proteins (Figure 1A), such as carboxypeptidase Y (CPY) (Trimble and Atkinson, 1986, Ballou *et al.*, 1990), the other is a mannan structure that consists of a long-branched mannose polymer (approximately 200 mannose residues) (Figure 1B), which is attached to many

proteins that are localized to the cell wall and periplasmic space such as invertase (Peat *et al.*, 1961, Ballou, 1974, Herscovics and Orlean, 1993). It is not clear why some glycoproteins forms mannan-structure and others do not. In mammalian cells, a complicated sequence of hydrolytic reactions takes place in the Golgi apparatus, called processing or trimming reactions, and may remove five mannose groups before some GlcNAc, Gal, sialic acid, and fucose residues are added (Schachter, 1991).

O*-glycosylation in *S. cerevisiae

In yeast, *O*-glycosylation is known as *O*-mannosylation, as it refers to the addition of mannoses to the polypeptide. *O*-mannosylation is known to play an important role in various biological processes, including protein stability (Lommel *et al.*, 2004, Weber *et al.*, 2004), protein secretion (Strahl-Bolsinger *et al.*, 1999, Proszynski *et al.*, 2004), cell wall integrity (Gentzsch and Tanner, 1996), and the budding process (Sanders *et al.*, 1999). *O*-mannosylation is initiated in the ER by the protein mannosyl transferase (Pmt) families. In 1993, *PMT* gene was cloned for the first time by Tanner and his colleagues in *S. cerevisiae* (Strahl-Bolsinger *et al.*, 1993). The purification of the Pmt was hindered by the extremely small amount and the great instability of the enzyme. Using an antibody, which inhibited the *in vitro* reaction, a sufficient immuno-positive, although enzymatically inactive, material was obtained for protein sequencing, and the *PMT1* gene was cloned. The transfer reaction of mannose to Ser/Thr residues of proteins by Pmts, using Dol-P-Man as a mannosyl donor (Orlean, 1990), is

evolutionally conserved in various eukaryotic organisms from fungi to human and found even in bacterial species (e.g., *Corynebacterium glutamicum*, and *Mycobacterium tuberculosis*) (Strahl-Bolsinger *et al.*, 1993, Martin-Blanco and Garcia-Bellido, 1996, Strahl-Bolsinger *et al.*, 1999, Willer *et al.*, 2003, Oka *et al.*, 2004, VanderVen *et al.*, 2005, Mahne *et al.*, 2006).

As shown in Figure 3A, Pmt1p–Pmt6p have been classified into three subfamilies, *PMT1*, *PMT2*, and *PMT4* (Willer *et al.*, 2003). Additionally, members of the *PMT1* subfamily (Pmt1p and Pmt5p) reportedly interact in pairs with members of the *PMT2* subfamily (Pmt2p and Pmt3p) to form heterodimeric complexes (Pmt1p–Pmt2p, Pmt3p–pmt5p) and the *PMT4* subfamily proteins form homomeric complexes (Pmt4p–Pmt4p) (Girrbach and Strahl, 2003). These complexes, which are essential for mannosyltransferase activity, have a different substrate specificity and catalyze the *O*-mannose transfer reaction differently in response to different acceptor protein substrates *in vivo* (Figure 3B) (Gentzsch and Tanner, 1997). The analysis of ten different secretory proteins in *pmt1*Δ–*pmt4*Δ mutants revealed that six of the proteins were mannosylated by Pmt1p or Pmt2p, and the other four by Pmt4p (Gentzsch and Tanner, 1997). Depletion of any one of the *PMT* genes is viable, although cells lacking multiple *PMT* genes exhibit severe defects. Different combinations of *pmt1*Δ–*pmt4*Δ were assayed by Gentzsch *et al*, and they reported that triple-mutants *pmt1*Δ *pmt2*Δ *pmt4*Δ or *pmt2*Δ *pmt3*Δ *pmt4*Δ were not viable, and many other double or triple combinations resulted in the abnormal growth (Gentzsch and Tanner, 1997).

O-linked modifications of mammalian proteins take place exclusively in the

Golgi apparatus (mucin-type glycan). An exception is *O*-mannosylation that was considered specific for yeast until 1997, when the first reports describing mammalian *O*-mannosylated proteins were published (Chiba *et al.*, 1997, Yuen *et al.*, 1997). Little is known about the mammalian *O*-mannosylation pathway. However, two *PMT* family homologues, *POMT1* and *POMT2*, have been identified as putative mannosylating enzymes (Jurado *et al.*, 1999, Willer *et al.*, 2002). POMT1 and POMT2 have been reported to be integral ER membrane proteins, especially POMT2 is specifically expressed in sperm (Willer *et al.*, 2002). A recent report by Manya *et al.* provides the first data suggesting Pomt1 and/or Pomt2 to have a mannosyltransferase activity. This activity required co-expression of POMT1 and POMT2 (Manya *et al.*, 2004). Mutations in the *POMT1* gene have been implicated in Walker-Warburg syndrome (WWS), a disorder characterized by congenital muscular dystrophy and brain and eye abnormalities (Beltran-Valero de Bernabe *et al.*, 2002, Currier *et al.*, 2005). These mutations result in defects of *O*-mannosylation (Akasaka-Manya *et al.*, 2006).

In yeast, the stepwise elongation of *O*-linked sugar chains that are transferred by Pmts takes place in the Golgi apparatus and is catalyzed by α-1,2-mannosyl transferases, the Ktr (killer toxin resistant) family, and by α-1,3-mannosyl transferases, Mnn1p (Figure 1C and Figure 10A) (Lussier *et al.*, 1999). Different from Pmts, these enzymes are type-II membrane proteins containing only one transmembrane spanning region, a short cytoplasmic N terminus, and a large luminal, catalytic C-terminal domain. In mammals, the enzyme POMGnT1 (Protein *O*-mannose-β-1,2-*N*-acetylglucosaminyl transferase) transfers, in the Golgi apparatus, a GlcNAc residue

from UDP-GlcNAc to form an α-1,2-bond with the protein-bound mannose (Yoshida *et al.*, 2001). The galactosyl and sialyl transferases required for further extensions have not yet been identified. Possible candidates are fukutin and FKRP (fukutin-related protein).

The role of *N*-glycan in protein folding and ER quality control systems

ERQC systems monitoring folding-status operate everywhere proteins are synthesized (Sitia and Braakman, 2003, Bukau *et al.*, 2006). ER-localized chaperones and modifying enzymes (e.g., heavy chain binding protein (BiP), calnexin, and protein disulphide isomerase (PDI)) require the retention of unfolded proteins in the ER and the transport of correct folding proteins to the secretory pathway. The current understanding of ERQC comes mostly from studies of the budding yeast and mammalian cells (Gething *et al.*, 1986, Knop *et al.*, 1993, Hampton *et al.*, 1996). To monitor and eliminate the aberrant proteins, each organism relies on multiple endoplasmic reticulum-associated degradation (ERAD) pathways (Figure 4).

N-glycan contributes to a correct folding of glycoproteins and involved in ERQC systems. ERQC participates in the correct protein synthesis. Moreover, ER quality control systems decrease cell toxicity and prevent cell death due to the accumulation of aberrantly folded proteins in the ER by removing misfolded proteins (Bucciantini *et al.*, 2002). ER molecular chaperones (e.g., heavy chain binding protein (BiP), calnexin, and protein disulphide isomerase (PDI)) facilitate the folding of newly synthesized proteins. Especially, *N*-glycan structure, $Glc_3Man_9GlcNAc_2$, is trimmed and

processed by glucosidase I, glucosidase II, and mannosidase I, converting it to $Man_8GlcNAc_2$ (Helenius and Aebi, 2001, Helenius and Aebi, 2004). In mammalian systems, the intermediate of the trimming process, $Glc_1Man_9GlcNAc_2$, is capable of interacting with the lectin-like molecular chaperone calnexin/calreticulin (Figure 5). This interaction promotes the correct folding of newly synthesized glycoproteins in the ER (Ellgaard *et al.*, 1999). Yeast *Saccharomyces cerevisiae* has an ortholog of calnexin, Cne1p. However, Cne1p activity is not essential for the folding of glycoprotein in yeast cells (Kostova and Wolf, 2005), even though Cne1p is capable of interact with $Glc_1Man_9GlcNAc_2$ structure *in vitro* (Xu *et al.*, 2004). A removal of the remaining glucose then frees the native-folded glycoprotein from the lectins so the glycoprotein can exit the ER. A prolonged retention in the ER results in a mannose trimming, and another lectin, known as EDEM, has been proposed to bind the Man_8-containining glycan and to target these misfolded glycoproteins for 26S proteasome-dependent degradation after retrotranslocation into the cytosol and ubiquitination (Fewell *et al.*, 2001, Oda *et al.*, 2003). These process are called ER-associated degradation (ERAD) (Kopito, 1997, Kostova and Wolf, 2003). Studies from budding yeast indicate that their diversity of ERAD pathways represent a basic conserved standard set (Meusser *et al.*, 2005, Bukau *et al.*, 2006). Higher eukaryotes differ by an expansion of components and pathways, presumably to satisfy the needs in more complex organisms. In budding yeast, three ERQC pathways have been described that can account for much of the organelle's needs. These are the ERAD-C (ER-associated degradation-Cytosol), ERAD-L (-Lumen), and ERAD-M (-Membrane) pathways that monitor folding of cytosolic, membrane, and

luminal domains of client proteins, respectively (see Figure. 9B). Two E3 ubiquitin ligases, Hrd1p and Doa10p, organize factors involved in substrate recognition, extraction, and ubiquitination for these pathways (Vashist *et al.*, 2001, Vashist and Ng, 2004, Carvalho *et al.*, 2006, Denic *et al.*, 2006, Gauss *et al.*, 2006).

In addition, some misfolded secretory proteins appear to be targeted to the vacuole and degraded in a vacuolar protease-dependent manner (post-ER degradation) (Jorgensen *et al.*, 1999, Arvan *et al.*, 2002, Coughlan *et al.*, 2004, Kruse *et al.*, 2006a, Kruse *et al.*, 2006b, Fujita *et al.*, 2007). In post-ER degradation, misfolded model proteins, which are degraded by vacuolar proteases, are targeted to the vacuole via two routes, namely, the Golgi-to-vacuole sorting pathway (Conibear and Stevens, 1998) and the autophagic pathway (Klionsky and Emr, 2000).

The role of *O*-glycan in ER quality control systems

Recently, Harty *et al*. reported that a model misfold protein, pro-α-factor mutant (mutant pαF), is *O*-mannosylated only in its misfolded status (Harty *et al.*, 2001). It has also been reported that a pro-region-deleted derivative of *Rhizopus niveus* aspartic proteinase-I (Δpro) are *O*-mannosylated by Pmt1p and/or Pmt2p (Nakatsukasa *et al.*, 2004). More specifically, Δpro takes *O*-mannosylation only when some components of ERAD machinery are abolished (Nakatsukasa *et al.*, 2004) and another ERAD substrate, the Kar2p signal sequence fused to simian virus 5 haemagglutinin neuraminidase (KHN), is also *O*-mannosylated by Pmt1p and/or Pmt2p when expressed in yeast cells

(Vashist *et al.*, 2001). The *O*-mannosylation of misfolded proteins such as mutant pαF and Δpro enhances their solubility, preventing them from aggregation in the ER (Nakatsukasa *et al.*, 2004). However, the degradation of mutant pαF and Δpro is not affected by deletion of *PMT1* or *PMT2* (Harty *et al.*, 2001, Nakatsukasa *et al.*, 2004). Therefore, it remains unclear if *O*-mannosylation of misfolded proteins plays an essential role in ERAD pathways.

The aim of this study

The purpose of the present study is to elucidate the physiological function of misfolded protein-specific *O*-mannosylation, which is executed by Pmt1p and Pmt2p, in the degradation of misfolded proteins. In Chapter I, I dissect the molecular function of *O*-mannosylation using model misfolded protein; HA-tagged Kar2p signal sequence fused to simian virus 5-haemagglutinin neuraminidase (KHNt). It has been reported that KHNt is a substrate for degradation by the ERAD-L pathway and that KHNt is *O*-mannosylated by Pmt1p and Pmt2p. I reveal that *O*-mannosylation of KHNt is required for ER-to-Golgi transport. In Chapter II, using model misfolded protein Gas1*p, I report that Gas1*p was not degraded proteasome-dependently and sorting to the vacuole in Pmt1p and Pmt2p defected cells. This result suggests that *O*-mannosylation of Gas1*p is essential for its ERAD-dependent degradation. In the last part of this thesis, I discuss the physiological function of misfolded protein-specific *O*-mannosylation.

MATERIALS AND METHODS

Escherichia coli strain

For standard DNA propagation the strain DH5α (F^-, *f*80, *lac*ZDM15, D [*lac*ZYA-argF] U169, *hsd*R17 [rK^-,mK^+], *rec*A1, *end*A1, *deo*R, *thi*-1, *sup*E44, *gyr*A96, *rel*A1, l-) was used.

Yeast strains

Yeast strains used in this study are listed in Table II. W303-1A (*MAT***a** *ade2-1 his3-11 leu2-3,112 trp1-1 ura3-1 can1-100*), BY4741 (*MAT***a** *his3*Δ*1 leu2*Δ*0 met15*Δ*0 ura3*Δ*0*), BY4742 (*MAT*α *his3*Δ*1 leu2*Δ*0 lys2*Δ*0 ura3*Δ*0*) and YJY1 (*MAT***a** *his3*Δ*1 leu2*Δ*0 met15*Δ*0 ura3*Δ*0* [S288C background]) were mainly used as wild-type cells (Sutton *et al.*, 1991, Brachmann *et al.*, 1998, Fujita *et al.*, 2006a).

Media

E. coli strains were grown in LB medium (1% Bacto-Tryptone (Difco, Detroit, Michigan, USA), 0.5% Bacto-Yeast extract (Difco), and 1% NaCl, pH 7.2) at 37˚C.

Yeast strains were grown in the YPAD medium (2% glucose, 2% Bacto-Peptone (Difco), 1% Bacto-Yeast Extract, and 0.02% adenine-sulfate). For auxotrophic selection, Synthetic Dextrose (SD) medium (2% glucose, 0.67% yeast nitrogen base without amino acids (Difco)) was used. SD was supplemented with 20–400 μg/ml of amino acids, adenine-sulfate and uracil, when necessary. For tryptophan and uracil auxotrophic selection, SDCA medium (2% glucose, 0.67% yeast nitrogen base without

amino acids, 0.5% casamino acid and 0.02% adenine-sulfate) was used. For spore formation, SPO medium (1% potassium acetate) was used. Metabolic labeling experiments using [^{35}S]-cysteine/methionine were carried out in synthetic medium with a low SO_4^{2-} concentration (0.17% yeast nitrogen base without amino acids and ammonium sulfate, 0.5% casamino acids, 5% glucose, nutritional supplements, and 200 μM ammonium sulfate) and synthetic medium lacking methionine, cysteine, and ammonium sulfate (0.17% yeast nitrogen base without amino acids and ammonium sulfate, 0.5% casamino acids, 5% glucose, and nutritional supplements without cysteine and methionine). For osmotic stabilization, each medium was supplemented with 300 mM KCl.

Transformation of *E. coli* cells

Transformation of *E. coli* cells was done according to the method of Hanahan (Hanahan, 1983). One hundred μl of competent cells (purchased from Toyobo, Osaka, Japan) were gradually thawed and mixed gently with 5 μl of DNA solution. After incubation for 30 min on ice, cells were heat-shocked at 42˚C for 1 min. Immediately 900 μl of SOC medium (2% Bacto-Tryptone, 0.5% Bacto-Yeast Extract, 10 mM NaCl, 2.5 mM KCl, 10 mM $MgSO_4$, 10 mM $MgCl_2$, and 20 mM glucose) was added. After incubation for 1 h at 37˚C, the culture medium was spread onto LB-Amp plate (LB medium containing 100 μg/ml ampicillin and 1.5% agar), allowed to cultivate overnight at 37˚C.

Preparation of plasmid DNA from *E. coli* cells

E. coli cells which contain plasmid DNA were cultured overnight in 2 ml of LB-Amp medium (LB medium containing 0.01% ampicillin). Plasmid DNA was extracted using QIAprep Spin Miniprep Kit (Qiagen, Hilden, Germany).

Transformation of *S. cerevisiae* cells

Transformation of *S. cerevisiae* cells was done according to the method of Gietz (Gietz *et al.*, 1995). Yeast cells were incubated in 1 ml YPAD medium overnight at 30˚C with shaking. The pre-cultured cells were diluted to 5 ml YPAD (~2.0 OD_{600}). The cells were grown for 2.5 h. Cells were harvested in the sterile plastic tubes at 3000 × *g* for 5 min and the pellet was collected. Then cells were suspended in 5 ml of sterile water and centrifuged again. The cell pellet was resuspended in 1 ml of 100 mM LiAc and transferred to a 1.5 ml microtube. The suspension was centrifuged at top speed for 15 sec and the supernatant was removed with a micropipette. The cells were resuspended to a final volume of 500 µl. Then 50 µl of the competent cells was added to the transformation mixture (240 µl of 50% PEG 4000, 36 µl of 1 M LiAc, 12.5 µl of carrier DNA (4 mg/ml), 57.5 µl of sterile water, and 5 µl of plasmid DNA) and mixed well. The suspension was incubated at 30˚C for 30 min and then heat-shocked at 42˚C for 20 min. The mixture was centrifuged and the supernatant was removed. The cell pellet was washed with 1 ml of sterile water and spread on a selective medium plate.

Disruption of genes in yeast

Disruption of genes in yeast was performed with one step gene disruption method as described (Longtine *et al.*, 1998). PCR was performed using pFA6a-*LEU2* and pFA6a-*His3MX* plasmids (Longtine *et al.*, 1998) as templates. Appropriate forward target gene-specific primer with 5'-CGGATCCCCGGGTTAATTAA-3' at the 3' end and reverse target gene-specific primer with 5'-GAATTCGAGCTCGTTTAAAC-3' at the 3' end were used. The PCR product was introduced to yeast host cells. The transformants were selected with appropriate auxotrophy, and checked for the insertion site with yeast colony PCR using one primer that annealed within the transformation module and the second primer that annealed to the target gene locus outside the region altered.

Tetrad dissection

Mating

Yeast haploid strains of mating types of **a** and α were mixed and cultured on a YPAD plate for 2 days at room temperature.

Sporulation

Sporulation was carried out using SPO plate. Diploid strain grown on YPAD plate was picked up with sterilized toothpick and transferred to a SPO plate and incubated for 2 days at room temperature. Sporulation was confirmed microscopically.

Dissection

A diploid strain of *S. cerevisiae* was cultured on SPO plate for 2 days at room temperature for sporulation. The sporulrated cells were suspended in sterilized water. Then, small amounts of Zymolyase 100T were added into the suspension and incubated for 1 min at room temperature. Zymolyase digests cell wall of ascus. The suspension was spotted on YPAD plates, and dried up under a laminar flow cabinet. Tetrad ascospore was dissected individually with micromanipulator under a microscope. The individual ascospore was cultured independently and assayed for auxotrophic markers and biological functions. *pep4Δ pmt1Δ pmt2Δ* and *vps38Δ pmt1Δ pmt2Δ* triple-mutant strains were obtained in this way.

Plasmids used in this study

The plasmids used were as follows. The pSM70 plasmid, which contains the yeast Kar2p signal sequence fused to simian virus 5 haemagglutinin neuraminidase, with an HA-tag inserted at the carboxyl-terminal; the KHNt expression vector, which was a gift from Davis Ng (National University of Singapore, Singapore) (Vashist *et al.*, 2001); and pMF848 (HA-tagged *prc1-1*, *URA3*), which is described elsewhere (Fujita *et al.*, 2006b). The HA-Gas1p expression plasmid, pHI101, and the HA-Gas1*p expression plasmid, pHI102, were constructed as follows. Plasmids pMF600 (*HA*-tagged *GAS1*, *URA3*) (Fujita *et al.*, 2006b) and pMF605 (*HA*-tagged *gas1-871,873*, *URA3*) (Fujita *et al.*, 2006b) were digested with *Bam*HI and *Sac*II. The fragments containing *haemagglutinin* (HA)-tagged *GAS1* and HA-tagged *gas1-871,873* were

ligated into pRS316 (*CEN/ARS*, *URA3*) (Sikorski and Hieter, 1989) to generate pHI101 (HA-tagged *GAS1*, *CEN/ARS*, *URA3*), and pHI102 (*HA*-tagged *gas1-871,873*, *CEN/ARS, URA3*), respectively. To construct plasmids expressing non-GPI-anchored HA-Gas1p (HA-sol-Gas1p) and HA-Gas1*p (HA-sol-Gas1*p), the plasmids pMF876 (*HA*-tagged sol-*GAS1*, *URA3*) (Fujita *et al.*, 2006b) and pMF874 (*HA*-tagged sol-*gas1-871,873*, *LEU2*) (Fujita *et al.*, 2006b) were digested with *Bam*HI and *Spe*I, and fragments encoding HA-tagged sol-Gas1p and HA-tagged sol-Gas1*p were ligated into pRS316 (*CEN/ARS*, *URA3*) to generate pHI118 (*HA*-tagged sol-*GAS1*, *CEN/ARS*, *URA3*) and pHI119 (*HA*-tagged sol-*gas1-871,873*, *CEN/ARS*, *URA3*), respectively.

Pulse-chase and immunoprecipitation experiments

Cells were grown to a logarithmic phase of growth in synthetic medium with low SO_4^{2-}. Then, 15 OD_{600} units of cells were washed and resuspended in 3 ml of the synthetic medium lacking methionine, cysteine, and ammonium sulfate. After 20–40 min of incubation at 30°C, cells were pulse-labeled with 30 μCi Pro-mix-L [^{35}S] *in vitro* cell labeling mix (GE Healthcare Life Sciences, Piscataway, NJ) for 10 min. The chase phase was initiated by the addition of 1/100 volume of chase cocktail (0.3% methionine, 0.3% cysteine, and 0.3 M ammonium sulfate). The chase was terminated by addition of NaF and NaN_3 to a final concentration of 10 mM each. Preparation of cell lysate, immunoprecipitation, and SDS–PAGE were performed as described previously (Okamoto *et al.*, 2006). For peptide *N*-glycanase F (PNGase F) digestion, samples were

resuspended in denaturing buffer (0.5% SDS and 40 mM dithiothreitol (DTT)) and boiled for 10 min. Next, reaction buffer (0.5 M sodium phosphate [pH 7.5], 1% NP-40, and protease inhibitor cocktail [Roche, Basel, Switzerland]) was added, and the reaction mixture was treated with 125 U of PNGase F (New England Biolabs, Herts, UK) for 3 h at 37°C. Molecular Imager FX software (Bio-Rad, Hercules, CA) was used for quantification of SDS–PAGE gel bands.

Protein extraction and immunoblot analysis

Yeast cells were grown to logarithmic phase. Next, 1.0–5.0 OD_{600} units of cells were washed twice, resuspended in 100 μl of TEGN buffer (50 mM Tris–HCl [pH 7.5], 100 mM NaCl, 1 mM EDTA, 1% (w/v) NP-40 and protease inhibitor cocktail (Roche)), and disrupted with glass beads. After removing cell debris by centrifugation, cell lysates were denatured with sample buffer (125 mM Tris–HCl [pH6.8], 4% SDS, 20% glycerol, and 3.1% DTT) for 5 min at 98°C. A protein spin concentrator (Orbital Biosciences, Topsfield, MA) was used to concentrate a culture broth of *ktr1*Δ *kre2*Δ *ktr3*Δ cells expressing HA-sol-Gas1p (YME335). The concentrated culture broth was denatured as described above. Samples were separated by SDS–PAGE using 7.5% acrylamide gels. Proteins were transferred to PVDF membranes and blocked in TTBS (25 mM Tris–HCl [pH 7.4], 150 mM NaCl, and 0.1% (v/v) Tween-20) containing 0.5% (w/v) skim milk. Gas1p was detected with anti-Gas1p polyclonal rabbit antiserum (1:2000; kindly provided by K. Hata, Eisai Co., Ltd., Tokyo, Japan) followed by

horseradish peroxidase (HRP)-conjugated anti-rabbit IgG antibody (1:2000; Invitrogen, Carlsbad, CA). HA-tagged protein was detected with anti-HA mouse monoclonal antibody 16B12 (1:10,000; Covance, Princeton, NJ), followed by HRP-conjugated goat anti-mouse IgG antibody (1:10,000). Immunoreactive bands were detected by chemiluminescence with ECL Plus reagents (GE Healthcare Life Sciences).

Cycloheximide (CHX) chase analysis

CHX-chase analysis for yeast cells was performed as described previously (Fujita *et al.*, 2006b). Briefly, overnight overnight cultures were inoculated into 5 ml of medium. Cells were grown to OD_{600}=1.0. After adding CHX (Nakalai Tesque, Kyoto, Japan) to a final concentration of 0.2 mg/ml, 5 OD_{600} unit of cells were removed at specific time points, suspended in NaF and NaN_3 to a final concentration of 10 mM each. The preparation of samples and immunoblotting were performed as described above (see "**protein extraction and immunoblot analysis**").

Sucrose density gradient analysis

Cell extracts expressing HA-sol-Gas1*p were prepared as described above (see "**Protein extraction and immunoblot analysis**"). The extracts were resuspended in 400 µl of TEG buffer (50 mM Tris–HCl [pH 7.5], 100 mM NaCl, 1 mM EDTA, and protease inhibitor cocktail (Roche)) and then solubilized for 30 min at 4°C by addition

of Triton X-100 to a final concentration of 1% (w/v). The suspension was centrifuged at 20,000 × *g* for 30 min to remove insoluble membranes. The supernatant (300 μg of protein) was loaded onto a 5–50% (w/v) sucrose gradient and centrifuged at 145,000 × *g* for 20 h at 4°C, after which 200 μl fractions were collected from the bottom of the gradient and denatured with the sample buffer. An aliquot (10 μl) of each fraction was separated by SDS–PAGE and analyzed by Immunoblotting using anti-HA antibody (1:8000), followed by HRP-conjugated anti-mouse IgG antibody (1:8000). Molecular masses were estimated by comparison of the migration of proteins with the following standards: ferritin (440 kDa), catalase (232 kDa), aldolase (158 kDa), and ovalbumin (43 kDa).

Analysis of protein aggregates

Protein aggregate analysis was done using non-ionic detergent as described by Spear *et al.* (Spear and Ng, 2005), with some modifications. Wild-type cells expressing KHNt (YME1445), *pmt1*Δ *pmt2*Δ cells expressing KHNt (YME1446) and *pep4*Δ *pmt1*Δ *pmt2*Δ cells expressing KHNt (YME1447) were grown to a logarithmic phase in SCD medium. Then, 5.0 OD_{600} units of cells were collected by centrifugation and cell extracts were prepared as described above (see "**Protein extraction and immunoblot analysis**"). Cell extracts resuspended in TEG buffer were solubilized for 60 min at 4˚C by the addition of Triton X-100 to a final concentration of 1% (w/v). Half of the solubilized total cell extract was kept at 4˚C. The remaining half was centrifuged at

20,000 × *g* for 30 min, the supernatant was removed, and the pellet was resuspended in TEG buffer. Finally, the total cell extract, supernatant, and pellet fractions were denatured with the sample buffer and 10 μl of each sample was resolved by SDS–PAGE.

CHAPTER I

O-mannosylation is required for ERAD dependent degradation of KHNt

I-1. Summary

To better understand the physiological function of *O*-mannosylation to misfolded proteins in ERQC systems in *S. cerevisiae*, I selected and analyzed a model misfolded protein HA-tagged Kar2p signal sequence fused to simian virus 5 haemagglutinin neuraminidase (KHNt) (Figure 6A). It is reported that KHNt is a substrate for degradation by the ERAD-L pathway, the substrate of which requires ER-to-Golgi transport to proteasome-dependent degradation, and that KHNt is *O*-mannosylated by Pmt1p and Pmt2p (Vashist *et al.*, 2001).

I found that in a *pmt1*Δ *pmt2*Δ double-mutant background, the degradation rate of KHNt is significantly decreased as compared to that of KHNt expressed in wild-type background cells. I further found that this defect of ERAD dependent degradation of KHNt in *pmt1*Δ *pmt2*Δ background is due to the severe aggregation of KHNt in the ER. Notably, KHNt expressed in *pmt1*Δ *pmt2*Δ double-mutant cells forms detergent-insoluble aggregates. Taken together, my data suggested that KHNt *O*-mannosylation alleviates its aggregation and facilitates ER-to-Golgi transport of KHNt in order to degrade it in an ERAD-L pathway-dependent manner.

I-2. Results

The rate of degradation of KHNt is significantly reduced in *pmt1*Δ *pmt2*Δ cells

To clarify the molecular role of *O*-mannosylation in ERQC, I examined whether *O*-mannosylation of KHNt, a misfolded model protein that is *O*-mannosylated in its misfolded status, has an essential role in its ERAD-dependent degradation using the cells lacking *PMT1* and *PMT2* genes because KHNt is *O*-mannosylated by Pmt1p and Pmt2p (Vashist *et al.*, 2001). As shown in Figure 6B, pulse-labeled KHNt protein expressed in wild-type cells is localized in the ER at the first time point (Figure 6B, p1 form at 0 min chase) and KHNt is lost rapidly after a 30 min chase and is nearly undetectable by 60 min. Stepwise increases in molecular weight were due to the elaboration of carbohydrates attached initially in the ER by Pmt1p and Pmt2p as reported previously (Vashist *et al.*, 2001). On the other hand, stepwise increases in molecular weight of KHNt were not observed in *pmt1*Δ *pmt2*Δ cells (Figure 6B right panel). The degradation rate of KHNt was decreased in *pmt1*Δ *pmt2*Δ cells as compared to that in wild-type cells (Figure 6B and C). Therefore, it is suggested that non-*O*-mannosylated KHNt could not be transported to the Golgi, which is essential for the degradation of ERAD-L substrates.

KHNt expressed in the cells lacking *PMT1* and *PMT2* forms severe aggregates in the ER

Because KHNt could not be degraded efficiently in proteasome dependent

manner via ERAD-L pathway in *pmt1*Δ *pmt2*Δ cells, I suspected that KHNt is defective in its transport from ER to Golgi due to the formation of severe aggregates of KHNt in the ER in *pmt1*Δ *pmt2*Δ mutant cells. To investigate this possibility, I fractionated KHNt expressed in wild-type and *pmt1*Δ *pmt2*Δ background cells using the sucrose density gradient and detergent fractionation assays. As shown in Figure 7A and B, a large amount of KHNt was observed in the bottom fraction of sucrose density gradient in *pmt1*Δ *pmt2*Δ mutant cells, indicating that KHNt was aggregated. In sucrose density gradient of wild-type cell lysates, I could not detect Golgi form of KHNt (see p2 form of Figure 6B). Since the previous report suggests that the Golgi form of KHNt is preferentially degraded in wild-type cells (Vashist *et al.*, 2001), it is reasonable that Golgi form of KHNt could not be detected presumably because of its small amount or degradation during fractionation step. In detergent-partition assay using TritonX-100, KHNt expressed in *pmt1*Δ *pmt2*Δ mutant cells showed a detergent-insoluble aggregated form (Figure 7C). These results indicate that the rate of degradation of KHNt was significantly reduced due to their severe aggregation in *pmt1*Δ *pmt2*Δ double-mutant cells.

I-3. Discussion

KHNt is one of the ERAD-L model substrates that take *O*-mannosylation, executed by Pmt1p and Pmt2p (Vashist *et al.*, 2001) as well as mutant pαF and Δpro proteins that take *O*-mannosylation, executed by Pmt1p and Pmt2p in their unfolded status (Nakatsukasa *et al.*, 2004). It has been reported that the modification of highly hydrophilic *O*-mannosyl sugar chains to mutant pαF and Δpro make them more soluble and alleviate their solubility (Nakatsukasa *et al.*, 2004). However, the defect in Pmt1p and Pmt2p activity does not affect the degradation rate of mutant pαF and Δpro. Thus, the physiological function of *O*-mannosylation in ERQC systems remains unclear. In this report, to better understand the physiological function of *O*-mannosylation in ERQC systems, I dissected the behavior of KHNt in the cell lacking both *PMT1* and *PMT2*. First, I found that in *pmt1*Δ *pmt2*Δ double-mutant cells, the degradation rate of KHNt is significantly decreased as compared to that in wild-type cells (Figure 6B and C). Second, KHNt forms severe aggregates in the ER when Pmt1p and Pmt2p are defective, suggesting that *O*-mannosylation of KHNt is essential for its ERAD-L dependent degradation and that the behavior of KHNt is different from that of mutant pαF or Δpro in *pmt1*Δ *pmt2*Δ cells.

Physiological role of *O*-mannosylation to KHNt in ERQC systems

In wild-type cells, KHNt is *O*-mannosylated by Pmt1p–Pmt2p complex. *O*-mannosylated KHNt can exit the ER and be targeted to proteasome via ERAD-L

pathway as shown in the schematic diagram of Figure 8A. In case of the cell lacking *PMT1* and *PMT2*, non-*O*-mannosylated KHNt could not exit the ER. In consequence, non-*O*-mannosylated KHNt forms severe aggregates in the ER (Figure 8B). Taken together, *O*-mannosylation in ERQC systems may have two reasonable physiological functions. First, *O*-mannosylation may function to increase the solubility of KHNt and prevent cell-toxicity due to the accumulation of aggregated KHNt in the ER. Second, *O*-mannosylation of KHNt functions as 'selection tag' in ERQC systems. For example, *O*-mannosylation, executed by Pmt1p and Pmt2p, may be specifically required for transport KHNt to the Golgi and for interaction with unidentified cargo receptors. From the standpoint of this hypothesis, the accumulation of aggregate KHNt in *pmt1*Δ *pmt2*Δ mutant cells will be a secondary effect due to the defect in ER-to-Golgi transport of KHNt.

In summary, I revealed the nature of misfolded protein-specific *O*-mannosylation. The detail mechanism and interplay of the unidentified factor should be clarified by further studies.

CHAPTER II

O-mannosylation is prerequisite for the proteasome-dependent degradation of the model ERAD substrate Gas1*p

II-1 summary

To further understand the physiological significance of *O*-mannosylation in ERQC systems, I studied the behavior of another model misfolded protein, Gas1*p. The glycosylphosphatidylinositol (GPI)-anchored protein Gas1p functions as a glucanosyltransferase on the plasma membrane and is modified by both *N*- and *O*-glycosylation (Mouyna *et al.*, 2000). We previously generated Gas1*p, a misfolded ERAD substrate, and demonstrated that deacylation of the GPI anchor is important for the degradation of Gas1*p (Fujita *et al.*, 2006b).

In the current study, I dissected the molecular role of *O*-mannosylation in degradation of misfolded proteins using Gas1*p and a non-GPI-anchored soluble version of Gas1*p (sol-Gas1*p). I found that Gas1*p is excessively *O*-mannosylated as compared to Gas1p. Pmt1p and Pmt2p, which are not responsible for *O*-mannosylation of correctly folded Gas1p, participate in *O*-mannosylation of Gas1*p. I further found that in cells lacking both Pmt1p and Pmt2p functions (*pmt1*Δ *pmt2*Δ), Gas1*p is transported to the vacuole via the endosomal sorting process, and degradation of Gas1*p shifts from a proteasome-dependent (ubiquitin/proteasome ERAD) to a vacuolar protease-dependent (post-ER degradation) pathway. These results support the idea that *O*-mannosylation of Gas1*p as catalyzed by Pmt1p and Pmt2p plays a crucial role in degradation of Gas1*p through the ERAD pathway, which is dependent on proteasome degradation, and that vacuolar protease-dependent degradation of Gas1*p is facilitated in *pmt1*Δ *pmt2*Δ double-mutant background cells.

II-2 Results

Gas1*p is an ERAD-L substrate

Gas1p is an *N*-glycosylated protein that contains 10 potential *N*-glycosylation sites (Asn-X-Ser/Thr) and is a highly *O*-mannosylated GPI-anchored protein (Vai *et al.*, 1991, Popolo and Vai, 1999). The misfolded form of Gas1p referred to as Gas1*p has a single amino acid substitution (G291R) (Figure 9A) and is degraded by the proteasome as an ERAD substrate (Fujita *et al.*, 2006b). Furthermore, in the pulse-chase experiment of Gas1*p, I observed a stepwise increase of molecular weight as chasing-period proceeds due to *N* and *O*-glycan elongation (unpublished data). I first addressed whether ER-to-Golgi trafficking is essential for the ERAD-dependent degradation of Gas1*p, as reported for some other misfolded proteins (ERAD-L substrate), including mutant carboxypeptidase Y (CPY*) and KHN (Vashist *et al.*, 2001, Taxis *et al.*, 2002), using *sec18-1* mutant, which has deficiency in ER-to-Golgi trafficking at the non-permissive temperature (37˚C) (Figure 9B). As shown in Figure 9C, the degradation rate of Gas1*p was significantly decreased at the non-permissive temperature. This result suggests that ER-to-Golgi trafficking is required for the efficient Gas1*p degradation and the Gas1*p is also an ERAD-L substrate.

Excessive *O*-mannosylation of Gas1*p in the ER

I next asked if there is a difference in the extent of *O*-mannosylation of HA-Gas1p and HA-Gas1*p by Pmts. To do this, I carried out experiments in the cells with

deletions of *KTR1, KRE2,* and *KTR3* (*ktr1*Δ *kre2*Δ *ktr3*Δ triple-mutant cells), genes that encode α-1,2-mannosyltranserases involved in addition of the second and third mannose residues of *O*-linked sugar chains (Figure 10A) and addition of outer chain mannose residues of *N*-glycan in the Golgi apparatus (Lussier *et al.*, 1997). Because Gas1p and Gas1*p take *O*-linked sugar chains elongation through their transport to the Golgi, the molecular weights of HA-Gas1p and HA-Gas1*p include the influence of *N*- and *O*-glycan elongation in Golgi apparatus. We compared the molecular weights of Gas1p and Gas1*p after digestion of *N*-glycan by PNGase F in *ktr1*Δ *kre2*Δ *ktr3*Δ triple-mutant cells. After digestion of *N*-glycan with PNGase F, the content of *O*-mannosylated Ser/Thr residues is reflected on the difference in molecular weight between Gas1p and Gas1*p. We previously reported that the amount of intracellular Gas1*p is less than that of Gas1p in the steady-sate cells, because of an ERAD-dependent rapid degradation of Gas1*p (Fujita *et al.*, 2006b). To detect a small difference in the gel mobility between Gas1p and Gas1*p, I applied 4 times concentrated cell lysate samples of HA-Gas1*p than those of HA-Gas1p. Prior to digestion with PNGase F, the molecular weight of HA-Gas1p was higher than that of HA-Gas1*p (Figure 10B, lanes 1 and 2). This difference in molecular weight was presumably due to differences in the extent of elongation of *N*-linked sugar chains. In other words, the *N*-linked sugar chains of the mature HA-Gas1p were modified completely via the post-ER secretory pathway, whereas the *N*-linked sugar chains of HA-Gas1*p were only partially modified in the Golgi apparatus. However, HA-Gas1*p had a higher molecular weight than HA-Gas1p after *N*-glycan digestion with PNGase F (Figure 10B, lanes 3 and 4). Because the cells

lack *KTR1*, *KRE2*, and *KTR3*, the differences in molecular weight between HA-Gas1p and HA-Gas1*p after the PNGase F digestion should reflect differences in *O*-linked first mannose content. These results suggest that HA-Gas1*p contains more *O*-mannosylated serine/threonine residues than HA-Gas1p.

Previous findings indicated that HA-Gas1*p is indeed modified with GPI (Fujita *et al.*, 2006b). Thus, I next examined whether excessive *O*-mannosylation of HA-Gas1*p depends on GPI modification using the same assay in conjunction with expression of non-GPI-attached Gas1p (HA-sol-Gas1p) and Gas1*p (HA-sol-Gas1*p), which were constructed by insertion of a stop codon just before the GPI attachment signal sequence (Figure 13A). Since the amount of intracellular HA-sol-Gas1*p is smaller than that of HA-sol-Gas1p per cell, I used 4 fold concentrated samples for HA-sol-Gas1*p using *ktr1*Δ *ker2*Δ *ktr3*Δ triple-mutant cells. After PNGase F treatment, HA-sol-Gas1*p had a higher molecular weight than those of secreted HA-sol-Gas1p and intracellular HA-sol-Gas1p (Figure 10C, lanes 4–6), indicating that not only GPI-anchored Gas1*p but also sol-Gas1*p (non-GPI-anchor attached Gas1*p) contains more *O*-mannosylated Ser/Thr residues than correctly folded Gas1p or sol-Gas1p.

Pmt1p and Pmt2p are responsible for *O*-mannosylation of Gas1*p

Because there are more *O*-mannosylated sites in both HA-Gas1*p and HA-sol-Gas1*p than those in HA-Gas1p and HA-sol-Gas1p, I next sought to determine if Gas1p and Gas1*p are *O*-mannosylated by different Pmt proteins using cells with

deletions of single *pmt* genes. Gas1p was under-glycosylated in *pmt4*Δ and *pmt6*Δ cells (Figure 11A) as reported previously (Gentzsch and Tanner, 1997), whereas HA-Gas1*p was under-glycosylated in *pmt1*Δ and *pmt2*Δ mutant cells (Figure 11B) as well as in *pmt4*Δ and *pmt6*Δ mutant cells. Moreover, HA-Gas1*p expressed in both *pmt1*Δ *pmt2*Δ and *pmt4*Δ *pmt6*Δ double-deletion mutant cells was more under-glycosylated than that expressed in either single deletion mutant strain (data not shown).

I next used this method to further investigate which Pmt proteins are responsible for the *O*-mannosylation of HA-sol-Gas1*p. Interestingly, I observed under-glycosylation of HA-sol-Gas1*p in *pmt1*Δ and *pmt2*Δ cells, whereas glycosylation of HA-sol-Gas1*p was not affected by the deletion of *PMT4* and *PMT6* genes (Figure 11C). The result that Pmt4p is not involved in the mannosylation of HA-sol-Gas1*p is consistent with a recent report that Pmt4p specifically mannosylates several transmembrane proteins and GPI-anchored proteins, including Fus1p and Gas1p, whereas non-transmembrane forms of Fus1p (FUSw/oTM^{ZZ}) and non-GPI-attached Gas1p (GAS1ΔGPI^{ZZ}) are not *O*-mannosylated by Pmt4p (Hutzler *et al.*, 2007). These observations also support that Pmt1p and Pmt2p participate in *O*-mannosylation of the misfolded proteins Gas1*p and sol-Gas1*p.

Gas1*p expressed in *pmt1*Δ *pmt2*Δ double-mutant cells is degraded by vacuolar protease

Because Gas1*p was *O*-mannosylated by Pmt1p and Pmt2p as well as by Pmt4p and Pmt6p, I suspected that the *O*-mannosylation of Gas1*p that is mediated by

Pmt1p and Pmt2p plays a different physiological role than that mediated by Pmt4p and Pmt6p. To address this possibility, I compared the rate of degradation of HA-Gas1*p in wild-type, *pmt1*Δ *pmt2*Δ, and *pmt4*Δ *pmt6*Δ cells. As shown in Figure 12 A and B, the rate of degradation of HA-Gas1*p was similar to that in wild-type, *pmt1*Δ *pmt2*Δ, and *pmt4*Δ *pmt6*Δ cells.

Gas1*p is degraded by the proteasome (Fujita *et al.*, 2006b). However, it is known that some misfolded soluble proteins exit the ER and are degraded in the vacuole instead (Jorgensen *et al.*, 1999, Arvan *et al.*, 2002, Coughlan *et al.*, 2004). To determine if HA-Gas1*p in *pmt* mutants is degraded by vacuolar proteases, I examined the kinetics of degradation of HA-Gas1*p in cells lacking a vacuolar protease (*pep4*Δ) and in cells lacking both vacuolar protease and protein *O*-mannosyltransferases (*pep4*Δ *pmt1*Δ *pmt2*Δ and *pep4*Δ *pmt4*Δ *pmt6*Δ). Notably, degradation of HA-Gas1*p was significantly delayed in *pep4*Δ *pmt1*Δ *pmt2*Δ cells (Figure 12 C and D), whereas degradation of HA-Gas1*p in *pep4*Δ cells was not affected as compared to wild-type cells, as shown in our previous report (Fujita *et al.*, 2006b). Furthermore, degradation of HA-Gas1*p expressed in *pep4*Δ *pmt4*Δ *pmt6*Δ cells was not delayed (Figure 12 C and D).

To further address a possible mechanism for the delay in degradation of HA-sol-Gas1*p, I performed a CHX-chase experiment for HA-sol-Gas1*p expressed in wild-type, *pep4*Δ, and *pep4*Δ *pmt1*Δ *pmt2*Δ cells. As shown in Figure 13 B and C, HA-sol-Gas1*p was stable in triple gene-disrupted cells (*pep4*Δ *pmt1*Δ *pmt2*Δ), in contrast to what was observed for wild-type and *pep4*Δ cells. These results strongly suggest that

the defect in *O*-mannosylation of Gas1*p, which is mediated by Pmt1p and Pmt2p, leads to vacuolar protease-dependent degradation of Gas1*p, which is independent of GPI-anchor modification.

Gas1*p forms a weakly aggregated oligomer in *pep4*Δ *pmt1*Δ *pmt2*Δ triple-mutant cells

The above observations prompted me to examine why HA-Gas1*p is degraded by vacuolar protease when expressed in *pmt1*Δ *pmt2*Δ cells but not when expressed in wild-type or *pmt4*Δ *pmt6*Δ cells (Figure 12 C and D). I suspected that HA-Gas1*p expressed in *pmt1*Δ *pmt2*Δ cells aggregates in the ER and that aggregated HA-Gas1*p can be transported to the vacuole to be degraded. This hypothesis is partially supported by the finding that *O*-mannosylation enhances solubility and suppresses aggregation of several *O*-mannosylated misfolded proteins, including mutant pαF and Δpro (Nakatsukasa *et al.*, 2004). Moreover, it was recently reported that when the aggregation-competent Z variant of human α-1 proteinase inhibitor (A1PiZ) is expressed in yeast cells, it is targeted to the vacuole (Kruse *et al.*, 2006a). To address whether HA-Gas1*p forms an aggregate in *O*-mannosylation defective cells, I monitored the level of aggregated HA-sol-Gas1*p derived from wild-type, *pep4*Δ, and *pep4*Δ *pmt1*Δ *pmt2*Δ cells separated by sucrose density centrifugation. GPI-anchored Gas1*p could not be fractionated on the sucrose density gradient, presumably because Gas1*p tends to be insoluble due to the lipid moiety of the GPI-anchor. Therefore, I used HA-sol-Gas1*p, which, like HA-Gas1*p, is *O*-mannosylated by Pmt1p and Pmt2p

(Figure 11C); is excessively *O*-mannosylated compared with sol-Gas1p (Figure 10B); and is stabilized when expressed in *pep4*Δ *pmt1*Δ *pmt2*Δ triple-mutant cells (Figure 13). As shown in Figure 14, sol-Gas1*p was not observed in the bottom fraction, different from other aggregated-prone misfolded proteins (Nakatsukasa *et al.*, 2004, Kruse *et al.*, 2006a). By contrast, I found that the distribution of HA-sol-Gas1*p expressed in *pep4*Δ *pmt1*Δ *pmt2*Δ cells was shifted slightly, appearing in a higher molecular weight fraction than it does in a wild-type background (Figure 14A). Especially, the relative amount of HA-sol-Gas1*p in *pep4Δ pmt1Δ pmt2Δ* triple-mutant cells in fraction 4–6 is increased as compared with those of wild-type and *pep4Δ* mutant cells (Fig. 14B; the region of horizontal bracket). This result suggests that HA-sol-Gas1*p does not aggregate severely, but does form a weakly aggregated oligomer (small aggregate) in *pmt1*Δ *pmt2*Δ double-mutant cells.

Degradation of CPY* is not affected by defects in Pmt1p or Pmt2p

It has been reported that a defect in the ERAD machinery facilitates the anterograde transport of CPY* such that CPY* is finally degraded by the vacuole-localized protease (Kincaid and Cooper, 2007) and that a defect in Pmt2p leads to activation of the unfolded protein response (Nakatsukasa *et al.*, 2004). Given these reports, I suspect that the vacuolar protease-dependent degradation of HA-Gas1*p is an indirect effect resulting from general ER stress caused by deletion of *PMT1* and *PMT2*. To investigate this possibility, I examined the degradation of CPY*, which has been

extensively studied as an ERAD substrate in yeast (Finger *et al.*, 1993, Knop *et al.*, 1996) and is modified at four sites by *N*-glycan but is not *O*-mannosylated. The kinetics of degradation of CPY*-HA were monitored in wild-type, *pep4*Δ and *pep4*Δ *pmt1*Δ *pmt2*Δ cells by CHX-chase analysis. I found that the degradation kinetics of CPY*-HA were the same in all three strains (Figure 15A and B), indicating that a defect in Pmt1p and Pmt2p does not affect the rate of degradation of non-*O*-mannosylated ERAD substrates. Therefore, the stabilization of Gas1*p might not result from general ER stress due to the *PMT* deletions but instead, might be attributable to a defect in *O*-mannosylation.

Gas1*p is targeted to the vacuole via endosomes in *pmt1*Δ *pmt2*Δ double-mutant cells

Previous studies reported that some misfolded proteins that are degraded by vacuolar proteases are targeted to vacuoles via two pathways (Figure 16), the Golgi-to-vacuole pathway (Holkeri and Makarow, 1998, Coughlan *et al.*, 2004, Kruse *et al.*, 2006a) and the autophagic pathway (Kamimoto *et al.*, 2006, Kruse *et al.*, 2006a, Fujita *et al.*, 2007, Mazon *et al.*, 2007). Because ER-to-Golgi trafficking of Gas1*p is required for proteasome-dependent degradation (Fujita *et al.*, 2006b), I hypothesized that Gas1*p is transported to the vacuole via the Golgi apparatus. To address this possibility, I analyzed the kinetics of degradation of HA-Gas1*p in *vps38* deletion mutant cells. Vps38p is a component of the Vps30 Complex II (Vps15p–Vps34p–Vps38p–Vps30p complex), which recruits and stimulates the phosphatidylinositol 3-kinase Vps34p

(Figure 16). Vps34p kinase activity in endosomal membranes is required for the proper sorting of some vacuole-targeted proteins from the Golgi to vacuoles (Odorizzi *et al.*, 2000). As shown in Figure 17, I found that degradation of HA-Gas1*p was significantly reduced in *vps38*Δ *pmt1*Δ *pmt2*Δ cells as compared to its degradation in wild-type or *vps38*Δ single-mutant cells. Furthermore, the degree of HA-Gas1*p stabilization in *vps38*Δ *pmt1*Δ *pmt2*Δ cells was similar to that of stabilization observed in *pep4*Δ *pmt1*Δ *pmt2*Δ cells (Figure 12C and D). This suggests that HA-Gas1*p enters the Golgi-to-vacuole pathway via endosome and that targeting of HA-Gas1*p to the vacuole depends on the *VPS30* complex II in *pmt1*Δ *pmt2*Δ cells (see Discussion).

II-3 Discussion

In this report, I dissected the role of *O*-mannosylation in the intracellular quality control machinery using the misfolded protein Gas1*p. I showed that Gas1*p is excessively *O*-mannosylated by Pmt1p and Pmt2p as compared to a correctly folded Gas1p. I also found that HA-Gas1*p is transported to the vacuole via the Golgi and endosome, and degraded by vacuolar proteases only when protein *O*-mannosylation, which is executed by Pmt1p and Pmt2p, is abolished. My data suggest that Pmt1p and Pmt2p are important for proteasome-dependent degradation of Gas1*p. In wild-type cells, Gas1*p is primarily degraded by ERAD pathway. The balance of the operated pathways could be regulated such that Gas1*p is degraded mainly by the vacuolar-dependent pathway when *PMT1* and *PMT2* are deleted, although it is still unclear if the contribution by ERAD pathway is completely abolished in these circumstances. Thus, I hypothesize that *O*-mannosylation by Pmt1p and Pmt2p is a key step in the targeting of Gas1*p for degradation via the proteasome-dependent ERAD pathway.

Excessive *O*-mannosylation of Gas1*p

ERAD substrates including mutant pαF and Δpro seem to be less soluble than correctly folded proteins (Nakatsukasa *et al.*, 2004). Mutant pαF, Δpro and KHNt proteins are modified with highly hydrophilic *O*-mannosyl sugar chains to make them more soluble. It is noteworthy that Gas1*p is not likely a solubility-reduced ERAD substrate because Gas1*p is highly glycosylated in the ER (the molecular weight of the

primary translated form of Gas1*p is 65 kDa and that of the glycosylated form is ~100 kDa) in contrast to other *O*-mannosylated misfolded proteins. In the experiment using *pep4Δ pmt1Δ* or *pep4Δ pmt2Δ* double-mutant cells, the degradation rate of Gas1*p is not reduced to the same extent as that of Gas1*p expressed in *pep4Δ pmt1Δ pmt2Δ* cells (unpublished data), presumably due to the compensation of defect in Pmt1p and/or Pmt2p functions by Pmt3p or Pmt5p (Gentzsch and Tanner, 1997). After co-translational *O*-mannosylation by Pmt4p and Pmt6p, Gas1*p-specific *O*-mannosylation, which is mediated by Pmt1p and Pmt2p, may occur post-translationally near the amino acid-substituted region (G291R), in which the polypeptide is unfolded and internal hydrophobic amino acids may be exposed on the surface of the protein. It is likely that *O*-mannoses are transferred to serine or threonine residues adjacent to the unfolded region of Gas1*p such that they alleviate aggregation due to hydrophobic interactions, helping to reduce or eliminate accumulation of misfolded proteins in the ER. Another possibility is that *O*-mannosylation mediated by Pmt1p and Pmt2p may act as a retrieval signal from the Golgi-to-ER in ERAD-L pathway (Vashist *et al.*, 2001, Nishikawa *et al.*, 2005, Fujita *et al.*, 2006b) or act as a tag for the recognition by ERAD machinery.

The transport pathway and sorting mechanism of Gas1*p to the vacuole

Two pathways have been reported for the transport of aggregated, misfolded proteins to the vacuole in yeast. One is the Golgi-to-vacuole sorting pathway (Holkeri and Makarow, 1998, Coughlan *et al.*, 2004, Kruse *et al.*, 2006a). The other is the

autophagic pathway (Kamimoto *et al.*, 2006, Kruse *et al.*, 2006a, Fujita *et al.*, 2007, Mazon *et al.*, 2007). Several reports suggest that the route of vacuolar targeting in post-ER degradation is substrate-specific. For Gas1*p transport to the vacuole, the Vps30p complex II is essential for Golgi-to-vacuole sorting via endosome. I could not clearly determine if the autophagic pathway is also used to target Gas1*p to the vacuole using the mutant cell of *ATG14*, which is an essential subunit of *VPS30* complex I (Vps15p–Vps34p–Atg14p–Vps30p complex) for autophagy, due to the severe growth defect of *atg14*Δ *pmt1*Δ *pmt2*Δ triple-mutant cells. However, the degradation kinetics of Gas1*p in *vps38*Δ *pmt1*Δ *pmt2*Δ cells resembled that in *pep4*Δ *pmt1*Δ *pmt2*Δ cells (Figure 12D and 17B) and Gas1*p was not so severely aggregated as compared with misfolded proteins which are transported to the vacuole via autophagic pathway; namely, A1PiZ, mutant fibrinogen, and mutant dysferlin, (Kruse *et al.*, 2006a, Kruse *et al.*, 2006b, Fujita *et al.*, 2007). Therefore, it is conceivable that a large proportion of Gas1*p is targeted to the vacuole via the Golgi apparatus in *pmt1*Δ *pmt2*Δ cells. I addressed whether Vps10p, a Golgi-to-vacuole sorting receptor of some vacuolar proteins, is involved in the sorting of Gas1*p, but found that the rate of degradation of Gas1*p was not reduced in *vps10*Δ or *vps10*Δ *pmt1*Δ *pmt2*Δ mutant cells (unpublished data). Taken together, the data suggest that Gas1*p and sol-Gas1*p may be sorted by a Golgi-to-vacuole sorting receptor other than Vps10p.

The aggregate formation of sol-Gas1*p in *pmt1*Δ *pmt2*Δ cells

I fractionated sol-Gas1*p by sucrose density gradient centrifugation and

observed a weakly aggregated sol-Gas1*p oligomer (Figure 14; it should be noted that GPI-anchored Gas1*p could not be fractionated). I could not clearly distinguish differences in aggregation of GPI-anchored Gas1*p in wild-type, *pep4*Δ, or *pep4*Δ *pmt1*Δ *pmt2*Δ cells. However, both sol-Gas1*p and Gas1*p contain more *O*-mannosylated serine/threonine residues than each of correctly folded forms (sol-Gas1p and Gas1p, respectively; Figure 10B and C) and as for Gas1*p, the degradation of sol-Gas1*p was delayed in *pep4*Δ *pmt1*Δ *pmt2*Δ cells (Figure 13). Therefore, it is conceivable that Gas1*p, which contains a GPI anchor, also behaves like sol-Gas1*p in *pep4*Δ *pmt1*Δ *pmt2*Δ triple-mutant cells.

In summary, I propose a model, explaining that excessive *O*-mannosylation of Gas1*p is essential role in its ERAD-dependent degradation. As shown in Figure 18A, in wild-type cells, excessively *O*-mannosylated Gas1*p can exit the ER and is targeted to ERAD via ERAD-L pathway and is degraded by 26S proteasome. On the other hand, underglycosylated Gas1*p, due to the defect of Pmt1p and Pmt2p, forms a weakly aggregated oligomer and is degraded vacuole proteases dependently after sending to the vacuole via Golgi apparatus (Figure 18B). Taken together, *O*-mannosylation that is executed by Pmt1p and Pmt2p to Gas1*p contributes to the alleviation of aggregation of Gas1*p and/or may function as a 'selection tag' in ERQC/ERAD mechanism.

GENERAL DISCUSSION

Overview of this thesis

In this thesis, I tried to figure out the physiological function of *O*-mannosylation in ERQC/ERAD systems by studying the several mutants involved in the *O*-mannosylation, ERQC, vacuole sorting, and vacuolar protease in *S. cerevisiae*. I selected two misfolded model proteins, KHNt and Gas1*p, that are degraded ERAD-dependently. In chapter I, I investigated the physiological roles of *O*-mannosylation using KHNt. *O*-mannosylation for KHNt, executed by Pmt1p and Pmt2p, is required for the ERAD-dependent degradation. The deficiency of Pmt1p and Pmt2p leads to form aggregates of KHNt in the ER lumen. I propose two possible scenarios in the section below for the reason why KHNt aggregates and accumulates in the ER.

In chapter II, I evaluated the behavior of other misfolded model protein, Gas1*p, in *O*-mannosylation-activity deficient cells. Gas1*p is a high-glycosylated protein and takes GPI-anchor modification, in spite of an aberrantly misfolded form of Gas1p. I found that Gas1*p is excessively *O*-mannosylated as compared to Gas1p. Pmt1p and Pmt2p, which are not responsible for the *O*-mannosylation of a correctly folded Gas1p, participate in *O*-mannosylation of Gas1*p, and that this excessive *O*-mannosyl modification is essential for the ERAD-dependent degradation of Gas1*p. Thus, I hypothesize that *O*-mannosylation by Pmt1p and Pmt2p is a key step in the targeting of Gas1*p for degradation via the proteasome-dependent ERAD pathway.

_O_-mannosylation in ERQC/ERAD: solubility-alleviate model

Although a physiological function of *O*-mannosylation in ERQC/ERAD is addressed in this study, the detail of molecular function of *O*-mannosylation remains unclear. I propose two models. The first model is a 'solubility-alleviate model', which means that the attachment of hydrophilic *O*-mannose to incompletely folded or misfolded proteins contributes to the avoidance of aggregate formation by increasing their solubility.

The degree to which sol-Gas1*p aggregated is significantly less than what was observed for another *O*-mannosylated misfolded protein KHNt in Pmt1p and Pmt2p defective cells (Figure 7 and 14). Because sol-Gas1*p is highly glycosylated and more soluble than other *O*-mannosylated misfolded proteins in their misfolded states, it seems reasonable that, different from other misfolded proteins, sol-Gas1*p was not present in a large amount in the fraction adjacent to the bottom fraction. Therefore, Gas1*p serves as a novel model for *O*-mannosylated misfolded protein, distinct from previously reported model proteins which take *O*-mannosylation under their misfolded status. Based on these differences between Gas1*p and KHNt, I propose a hypothesis that misfolded proteins that are *O*-mannosylated in their misfolded status can be classified into at least two classes in view of the degree of aggregation. Proteins in the first class of misfolded proteins, including KHNt, accumulate as a large aggregate in the ER when both *PMT1* and *PMT2* are defective. Proteins in the second class of misfolded proteins, including Gas1*p, form small aggregated oligomers but can exit the ER. However, it remains

unclear whether the degradation of previously reported two misfolded proteins Δpro and mutant-pαF, which are *O*-mannosylated under their misfolded status, are subjected to vacuolar proteases-dependent degradation when the function of Pmt1p and Pmt2p is abolished, because mutant pαF has been used as a model misfolded protein only for the *in vitro* ERAD assay system (McCracken and Brodsky, 1996, Pilon *et al.*, 1997, Harty *et al.*, 2001), and because Δpro is mannosylated only when the component of ERAD machinery is deleted (for example, in *der1*Δ or *cue1*Δ mutant) (Nakatsukasa *et al.*, 2004).

_O_-mannosylation in ERQC/ERAD: selection-tag model

The second model is a 'selection-tag model'. As described in Chapter I and II, under the circumstance of defect in both Pmt1p and Pmt2p, KHNt accumulates in the ER and Gas1*p is transported to the vacuole. These results raise the possibility, distinct from a 'solubility-alleviate model', that the *O*-mannosylation of KHN may function as a tag to exiting the ER and anterograde trafficking to the Golgi, and that an excessive *O*-mannosylation of Gas1*p may function as Golgi-to-ER retrieval signal. I am currently exploring this possibility. Although still speculative, lectin cargo receptors may be involved in misfold protein-specific ER-to-Golgi trafficking in yeast cells, like ERGIC-53 and VIP36, which capture the glycoprotein and mediate ER-to-Golgi trafficking in mammalian cells. Whether the ER-to-Golgi trafficking of misfolded proteins is essential for its degradation remains unclear in mammalian cells. However it is reported that a

part of the overexpressed model mammalian ERAD substrate, VSV-G ts045, escapes the ER and are transported to the Golgi, then retrieved to the ER in mammalian cells (Hammond and Helenius, 1994), and that the overexpression of Golgi α-1,2-mannosidase IA, IB, and IC accelerates ERAD-dependent degradation of misfolded human α-1-antitrypsin variant null Hong Kong (NHK) in mammalian cells (Hosokawa *et al.*, 2007). Therefore, it is likely that ERAD-L pathway, similar to yeast system, may function in mammalian ERQC/ERAD systems.

Perspectives

My results on the *O*-mannosylation of the misfolded proteins KHNt and Gas1*p suggest that *O*-mannosylation of proteins during proteasome-dependent degradation via the ERAD pathway serves as a component of the protein quality control machinery in *S. cerevisiae*. Such a mechanism has not been described in higher eukaryotes, but it is known that mammals also have protein *O*-mannosyltransferases and several *O*-glycosyltransferases in the ER (Spiro, 2002), suggesting that these transferases, like yeast Pmts, may participate in ERQC systems. Continued research on the role of *O*-mannosylation in the ER quality control systems of other *O*-mannosylated misfolded ERAD substrates will help clarify the detail of molecular mechanism of *O*-mannosylation in ERQC systems.

Although I elucidate the physiological function of *O*-mannosylation in ERQC/ERAD systems, there are numerous substrates that are not *O*-mannosylated but nevertheless degraded efficiently by ERAD. Thus, *O*-mannosylation may play

differential roles depending on the specific substrate but cannot serve as general signals. I found that the excessive *O*-mannosylation of KHNt and Gas1*p by Pmt1p and Pmt2p is important for the proteasome-dependent degradation. However several questions remained unsolved. For example, does Pmt1p–Pmt2p complex or additional other factors recognize unfolded region of misfolded proteins? Which Ser/Thr sites in KHNt and Gas1*p are specifically *O*-mannosylated by Pmt1p and Pmt2p? Are there any lectin-like receptors, which can recognize misfolded protein-specific *O*-mannosylation? Further studies to address these questions are necessary to understand better the molecular function of *O*-mannosylation of misfolded proteins in ERQC/ERAD systems.

ACKNOWLEDGEMENTS

This work was carried out at the Research Institute of Cell Engineering, National institute of Advanced Industrial Science and Technology (AIST), during 2005–2007. I would like to express my sincere gratitude to Dr Yoshifumi Jigami, Senior Researcher of the Research Institute of Cell Engineering, AIST, for his excellent scientific guidance and for his constant support and encouragement over these years. Working under his supervision has been a pleasure, and a valuable learning experience.

I am indebted to my committee members, Dr. Hideko Urushibara, Dr. Yoshihiro Shiraiwa, and Dr. Kenjiro Yoshimura, Graduate School of Life and Environmental Sciences, the University of Tsukuba. I appreciate the major time and effort they all contributed to improve this thesis.

I would like to acknowledge to the continuous guidance and helpful discussions of Dr. Takehiko Yoko-o, the Research Institute of Cell Engineering, AIST. My sincere gratitude to Dr. Takuji Oka, Mr. Toshihiko Kitajima, Dr. Morihisa Fujita Dr. Yasunori Chiba, and Dr. Yoh-ichi Shimma, group members of our laboratory, for guidance with experiments and helpful discussions.

I am grateful to Dr. Davis Ng (National University of Singapore, Singapore) for providing the pSM70 plasmid (KHNt expression vector); to Dr. Shu-ichi Nishikawa (Nagoya University, Nagoya, Japan) for the pUC18-Mfα plasmid; to Dr. Kazutoshi Mori (Kyoto University, Kyoto, Japan) for the UPR reporter assay plasmid (pSCZ-Y); and to Dr. Katsura Hata (Eisai Co.) for the anti-Gas1p peptide polyclonal antibody.

Finally, I would like to thank my families and my friends for their continuous encouragement and support of my research.

Tsukuba, March 2008

REFERENCES

AKASAKA-MANYA, K., MANYA, H., NAKAJIMA, A., KAWAKITA, M. & ENDO, T. (2006) Physical and functional association of human protein *O*-mannosyltransferases 1 and 2. *J Biol Chem,* 281**,** 19339-45.

ARVAN, P., ZHAO, X., RAMOS-CASTANEDA, J. & CHANG, A. (2002) Secretory pathway quality control operating in Golgi, plasmalemmal, and endosomal systems. *Traffic,* 3**,** 771-80.

BALLOU, C. E. (1974) Some aspects of the structure, immunochemistry, and genetic control of yeast mannans. *Adv Enzymol Relat Areas Mol Biol,* 40**,** 239-70.

BALLOU, L., HERNANDEZ, L. M., ALVARADO, E. & BALLOU, C. E. (1990) Revision of the oligosaccharide structures of yeast carboxypeptidase Y. *Proc Natl Acad Sci U S A,* 87**,** 3368-72.

BELTRAN-VALERO DE BERNABE, D., CURRIER, S., STEINBRECHER, A., CELLI, J., VAN BEUSEKOM, E., VAN DER ZWAAG, B., KAYSERILI, H., MERLINI, L., CHITAYAT, D., DOBYNS, W. B., CORMAND, B., LEHESJOKI, A. E., CRUCES, J., VOIT, T., WALSH, C. A., VAN BOKHOVEN, H. & BRUNNER, H. G. (2002) Mutations in the *O*-mannosyltransferase gene *POMT1* give rise to the severe neuronal migration disorder Walker-Warburg syndrome. *Am J Hum Genet,* 71**,** 1033-43.

BRACHMANN, C. B., DAVIES, A., COST, G. J., CAPUTO, E., LI, J., HIETER, P. & BOEKE, J. D. (1998) Designer deletion strains derived from Saccharomyces cerevisiae S288C: a useful set of strains and plasmids for PCR-mediated gene disruption and other applications. *Yeast,* 14**,** 115-32.

BUCCIANTINI, M., GIANNONI, E., CHITI, F., BARONI, F., FORMIGLI, L., ZURDO, J., TADDEI, N., RAMPONI, G., DOBSON, C. M. & STEFANI, M. (2002) Inherent toxicity of aggregates implies a common mechanism for protein misfolding diseases. *Nature,* 416**,** 507-11.

BUKAU, B., WEISSMAN, J. & HORWICH, A. (2006) Molecular chaperones and protein quality control. *Cell,* 125**,** 443-51.

BURDA, P. & AEBI, M. (1999) The dolichol pathway of *N*-linked glycosylation. *Biochim Biophys Acta,* 1426**,** 239-57.

CARVALHO, P., GODER, V. & RAPOPORT, T. A. (2006) Distinct ubiquitin-ligase complexes define convergent pathways for the degradation of ER proteins. *Cell,* 126**,** 361-73.

CHIBA, A., MATSUMURA, K., YAMADA, H., INAZU, T., SHIMIZU, T., KUSUNOKI, S., KANAZAWA, I., KOBATA, A. & ENDO, T. (1997) Structures of sialylated *O*-linked oligosaccharides of bovine peripheral nerve alpha-dystroglycan. The role of a novel *O*-mannosyl-type oligosaccharide in the binding of alpha-dystroglycan with laminin. *J Biol Chem,* 272**,** 2156-62.

CONIBEAR, E. & STEVENS, T. H. (1998) Multiple sorting pathways between the late Golgi and the vacuole in yeast. *Biochim Biophys Acta,* 1404**,** 211-30.

COUGHLAN, C. M., WALKER, J. L., COCHRAN, J. C., WITTRUP, K. D. & BRODSKY, J. L. (2004) Degradation of mutated bovine pancreatic trypsin inhibitor in the yeast vacuole suggests post-endoplasmic reticulum protein quality control. *J Biol Chem,* 279**,** 15289-97.

CURRIER, S. C., LEE, C. K., CHANG, B. S., BODELL, A. L., PAI, G. S., JOB, L., LAGAE, L. G., AL-GAZALI, L. I., EYAID, W. M., ENNS, G., DOBYNS, W. B. & WALSH, C. A. (2005) Mutations in *POMT1* are found in a minority of patients with Walker-Warburg syndrome. *Am J Med Genet A,* 133**,** 53-7.

DENIC, V., QUAN, E. M. & WEISSMAN, J. S. (2006) A luminal surveillance complex that selects misfolded glycoproteins for ER-associated degradation. *Cell,* 126**,** 349-59.

ELLGAARD, L., MOLINARI, M. & HELENIUS, A. (1999) Setting the standards: quality control in the secretory pathway. *Science,* 286**,** 1882-8.

FEWELL, S. W., TRAVERS, K. J., WEISSMAN, J. S. & BRODSKY, J. L. (2001) The action of molecular chaperones in the early secretory pathway. *Annu Rev Genet,* 35**,** 149-91.

FINGER, A., KNOP, M. & WOLF, D. H. (1993) Analysis of two mutated vacuolar proteins reveals a degradation pathway in the endoplasmic reticulum or a related compartment of yeast. *Eur J Biochem,* 218**,** 565-74.

FUJITA, E., KOUROKU, Y., ISOAI, A., KUMAGAI, H., MISUTANI, A., MATSUDA, C., HAYASHI, Y. K. & MOMOI, T. (2007) Two endoplasmic reticulum-associated degradation (ERAD) systems for the novel variant of the mutant dysferlin: ubiquitin/proteasome ERAD (I) and autophagy/lysosome ERAD (II).

Hum Mol Genet, 16**,** 618-29.

FUJITA, M., UMEMURA, M., YOKO-O, T. & JIGAMI, Y. (2006a) *PER1* is required for GPI-phospholipase A2 activity and involved in lipid remodeling of GPI-anchored proteins. *Mol Biol Cell,* 17**,** 5253-64.

FUJITA, M., YOKO-O, T. & JIGAMI, Y. (2006b) Inositol deacylation by Bst1p is required for the quality control of glycosylphosphatidylinositol-anchored proteins. *Mol Biol Cell,* 17**,** 834-50.

GAUSS, R., SOMMER, T. & JAROSCH, E. (2006) The Hrd1p ligase complex forms a linchpin between ER-lumenal substrate selection and Cdc48p recruitment. *Embo J,* 25**,** 1827-35.

GENTZSCH, M. & TANNER, W. (1996) The *PMT* gene family: protein *O*-glycosylation in *Saccharomyces cerevisiae* is vital. *EMBO J,* 15**,** 5752-9.

GENTZSCH, M. & TANNER, W. (1997) Protein-*O*-glycosylation in yeast: protein-specific mannosyltransferases. *Glycobiology,* 7**,** 481-6.

GETHING, M. J., MCCAMMON, K. & SAMBROOK, J. (1986) Expression of wild-type and mutant forms of influenza hemagglutinin: the role of folding in intracellular transport. *Cell,* 46**,** 939-50.

GIETZ, R. D., SCHIESTL, R. H., WILLEMS, A. R. & WOODS, R. A. (1995) Studies on the transformation of intact yeast cells by the LiAc/SS-DNA/PEG procedure. *Yeast,* 11**,** 355-60.

GIRRBACH, V. & STRAHL, S. (2003) Members of the evolutionarily conserved *PMT* family of protein *O*-mannosyltransferases form distinct protein complexes among themselves. *J Biol Chem,* 278**,** 12554-62.

HAMMOND, C. & HELENIUS, A. (1994) Quality control in the secretory pathway: retention of a misfolded viral membrane glycoprotein involves cycling between the ER, intermediate compartment, and Golgi apparatus. *J Cell Biol,* 126**,** 41-52.

HAMPTON, R. Y., GARDNER, R. G. & RINE, J. (1996) Role of 26S proteasome and *HRD* genes in the degradation of 3-hydroxy-3-methylglutaryl-CoA reductase, an integral endoplasmic reticulum membrane protein. *Mol Biol Cell,* 7**,** 2029-44.

HANAHAN, D. (1983) Studies on transformation of *Escherichia coli* with plasmids. *J Mol Biol,* 166**,** 557-80.

HARTY, C., STRAHL, S. & ROMISCH, K. (2001) *O*-mannosylation protects mutant alpha-factor precursor from endoplasmic reticulum-associated degradation. *Mol*

Biol Cell, 12**,** 1093-101.

HASELBECK, A. & TANNER, W. (1982) Dolichyl phosphate-mediated mannosyl transfer through liposomal membranes. *Proc Natl Acad Sci U S A,* 79**,** 1520-4.

HELENIUS, A. & AEBI, M. (2001) Intracellular functions of *N*-linked glycans. *Science,* 291**,** 2364-9.

HELENIUS, A. & AEBI, M. (2004) Roles of *N*-linked glycans in the endoplasmic reticulum. *Annu Rev Biochem,* 73**,** 1019-49.

HELENIUS, J., NG, D. T., MAROLDA, C. L., WALTER, P., VALVANO, M. A. & AEBI, M. (2002) Translocation of lipid-linked oligosaccharides across the ER membrane requires Rft1 protein. *Nature,* 415**,** 447-50.

HERSCOVICS, A. & ORLEAN, P. (1993) Glycoprotein biosynthesis in yeast. *Faseb J,* 7**,** 540-50.

HERSCOVICS, A. (1999) Processing glycosidases of *Saccharomyces cerevisiae*. *Biochim Biophys Acta,* 1426**,** 275-85.

HOLKERI, H. & MAKAROW, M. (1998) Different degradation pathways for heterologous glycoproteins in yeast. *FEBS Lett,* 429**,** 162-6.

HOSOKAWA, N., YOU, Z., TREMBLAY, L. O., NAGATA, K. & HERSCOVICS, A. (2007) Stimulation of ERAD of misfolded null Hong Kong alpha1-antitrypsin by Golgi alpha1,2-mannosidases. *Biochem Biophys Res Commun,* 362**,** 626-32.

HUFFAKER, T. C. & ROBBINS, P. W. (1982) Temperature-sensitive yeast mutants deficient in asparagine-linked glycosylation. *J Biol Chem,* 257**,** 3203-10.

HUTZLER, J., SCHMID, M., BERNARD, T., HENRISSAT, B. & STRAHL, S. (2007) Membrane association is a determinant for substrate recognition by *PMT4* protein *O*-mannosyltransferases. *Proc Natl Acad Sci U S A,* 104**,** 7827-32.

JORGENSEN, M. U., EMR, S. D. & WINTHER, J. R. (1999) Ligand recognition and domain structure of Vps10p, a vacuolar protein sorting receptor in *Saccharomyces cerevisiae*. *Eur J Biochem,* 260**,** 461-9.

JURADO, L. A., COLOMA, A. & CRUCES, J. (1999) Identification of a human homolog of the *Drosophila* rotated abdomen gene (*POMT1*) encoding a putative protein *O*-mannosyl-transferase, and assignment to human chromosome 9q34.1. *Genomics,* 58**,** 171-80.

KAMIMOTO, T., SHOJI, S., HIDVEGI, T., MIZUSHIMA, N., UMEBAYASHI, K., PERLMUTTER, D. H. & YOSHIMORI, T. (2006) Intracellular inclusions

containing mutant alpha1-antitrypsin Z are propagated in the absence of autophagic activity. *J Biol Chem,* 281**,** 4467-76.

KAWASAKI, T. (2003) [Glycobiology basics: glycoproteins]. *Tanpakushitsu Kakusan Koso,* 48**,** 910-5.

KELLEHER, D. J., KARAOGLU, D., MANDON, E. C. & GILMORE, R. (2003) Oligosaccharyltransferase isoforms that contain different catalytic *STT3* subunits have distinct enzymatic properties. *Mol Cell,* 12**,** 101-11.

KELLEHER, D. J. & GILMORE, R. (2006) An evolving view of the eukaryotic oligosaccharyltransferase. *Glycobiology,* 16**,** 47R-62R.

KINCAID, M. M. & COOPER, A. A. (2007) Misfolded Proteins Traffic from the Endoplasmic Reticulum (ER) Due to ER Export Signals. *Mol Biol Cell,* 18**,** 455-63.

KLIONSKY, D. J. & EMR, S. D. (2000) Autophagy as a regulated pathway of cellular degradation. *Science,* 290**,** 1717-21.

KNAUER, R. & LEHLE, L. (1999) The oligosaccharyltransferase complex from *Saccharomyces cerevisiae*. Isolation of the *OST6* gene, its synthetic interaction with *OST3*, and analysis of the native complex. *J Biol Chem,* 274**,** 17249-56.

KNOP, M., SCHIFFER, H. H., RUPP, S. & WOLF, D. H. (1993) Vacuolar/lysosomal proteolysis: proteases, substrates, mechanisms. *Curr Opin Cell Biol,* 5**,** 990-6.

KNOP, M., HAUSER, N. & WOLF, D. H. (1996) *N*-Glycosylation affects endoplasmic reticulum degradation of a mutated derivative of carboxypeptidase yscY in yeast. *Yeast,* 12**,** 1229-38.

KOPITO, R. R. (1997) ER quality control: the cytoplasmic connection. *Cell,* 88**,** 427-30.

KOSTOVA, Z. & WOLF, D. H. (2003) For whom the bell tolls: protein quality control of the endoplasmic reticulum and the ubiquitin-proteasome connection. *EMBO J,* 22**,** 2309-17.

KOSTOVA, Z. & WOLF, D. H. (2005) Importance of carbohydrate positioning in the recognition of mutated CPY for ER-associated degradation. *J Cell Sci,* 118**,** 1485-92.

KRUSE, K. B., BRODSKY, J. L. & MCCRACKEN, A. A. (2006a) Characterization of an ERAD gene as *VPS30/ATG6* reveals two alternative and functionally distinct protein quality control pathways: one for soluble Z variant of human alpha-1

proteinase inhibitor (A1PiZ) and another for aggregates of A1PiZ. *Mol Biol Cell,* 17**,** 203-12.

KRUSE, K. B., DEAR, A., KALTENBRUN, E. R., CRUM, B. E., GEORGE, P. M., BRENNAN, S. O. & MCCRACKEN, A. A. (2006b) Mutant fibrinogen cleared from the endoplasmic reticulum via endoplasmic reticulum-associated protein degradation and autophagy: an explanation for liver disease. *Am J Pathol,* 168**,** 1299-308; quiz 1404-5.

LEHLE, L., STRAHL, S. & TANNER, W. (2006) Protein glycosylation, conserved from yeast to man: a model organism helps elucidate congenital human diseases. *Angew Chem Int Ed Engl,* 45**,** 6802-18.

LOMMEL, M., BAGNAT, M. & STRAHL, S. (2004) Aberrant processing of the *WSC* family and Mid2p cell surface sensors results in cell death of *Saccharomyces cerevisiae O*-mannosylation mutants. *Mol Cell Biol,* 24**,** 46-57.

LONGTINE, M. S., MCKENZIE, A., 3RD, DEMARINI, D. J., SHAH, N. G., WACH, A., BRACHAT, A., PHILIPPSEN, P. & PRINGLE, J. R. (1998) Additional modules for versatile and economical PCR-based gene deletion and modification in Saccharomyces cerevisiae. *Yeast,* 14**,** 953-61.

LUSSIER, M., SDICU, A. M., BUSSEREAU, F., JACQUET, M. & BUSSEY, H. (1997) The Ktr1p, Ktr3p, and Kre2p/Mnt1p mannosyltransferases participate in the elaboration of yeast *O*- and *N*-linked carbohydrate chains. *J Biol Chem,* 272**,** 15527-31.

LUSSIER, M., SDICU, A. M. & BUSSEY, H. (1999) The *KTR* and *MNN1* mannosyltransferase families of *Saccharomyces cerevisiae*. *Biochim Biophys Acta,* 1426**,** 323-34.

MAHNE, M., TAUCH, A., PUHLER, A. & KALINOWSKI, J. (2006) The *Corynebacterium glutamicum* gene *pmt* encoding a glycosyltransferase related to eukaryotic protein-*O*-mannosyltransferases is essential for glycosylation of the resuscitation promoting factor (Rpf2) and other secreted proteins. *FEMS Microbiol Lett,* 259**,** 226-33.

MANYA, H., CHIBA, A., YOSHIDA, A., WANG, X., CHIBA, Y., JIGAMI, Y., MARGOLIS, R. U. & ENDO, T. (2004) Demonstration of mammalian protein *O*-mannosyltransferase activity: coexpression of *POMT1* and *POMT2* required for enzymatic activity. *Proc Natl Acad Sci U S A,* 101**,** 500-5.

MARTIN-BLANCO, E. & GARCIA-BELLIDO, A. (1996) Mutations in the rotated abdomen locus affect muscle development and reveal an intrinsic asymmetry in *Drosophila*. *Proc Natl Acad Sci U S A,* 93**,** 6048-52.

MAZON, M. J., ERASO, P. & PORTILLO, F. (2007) Efficient degradation of misfolded mutant Pma1 by endoplasmic reticulum-associated degradation requires Atg19 and the Cvt/autophagy pathway. *Mol Microbiol,* 63**,** 1069-77.

MCCRACKEN, A. A. & BRODSKY, J. L. (1996) Assembly of ER-associated protein degradation *in vitro*: dependence on cytosol, calnexin, and ATP. *J Cell Biol,* 132**,** 291-8.

MEUSSER, B., HIRSCH, C., JAROSCH, E. & SOMMER, T. (2005) ERAD: the long road to destruction. *Nat Cell Biol,* 7**,** 766-72.

MOUYNA, I., FONTAINE, T., VAI, M., MONOD, M., FONZI, W. A., DIAQUIN, M., POPOLO, L., HARTLAND, R. P. & LATGE, J. P. (2000) Glycosylphosphatidylinositol-anchored glucanosyltransferases play an active role in the biosynthesis of the fungal cell wall. *J Biol Chem,* 275**,** 14882-9.

NAKATSUKASA, K., OKADA, S., UMEBAYASHI, K., FUKUDA, R., NISHIKAWA, S. & ENDO, T. (2004) Roles of *O*-mannosylation of aberrant proteins in reduction of the load for endoplasmic reticulum chaperones in yeast. *J Biol Chem,* 279**,** 49762-72.

NISHIKAWA, S., BRODSKY, J. L. & NAKATSUKASA, K. (2005) Roles of molecular chaperones in endoplasmic reticulum (ER) quality control and ER-associated degradation (ERAD). *J Biochem (Tokyo),* 137**,** 551-5.

ODA, Y., HOSOKAWA, N., WADA, I. & NAGATA, K. (2003) EDEM as an acceptor of terminally misfolded glycoproteins released from calnexin. *Science,* 299**,** 1394-7.

ODORIZZI, G., BABST, M. & EMR, S. D. (2000) Phosphoinositide signaling and the regulation of membrane trafficking in yeast. *Trends Biochem Sci,* 25**,** 229-35.

OKA, T., HAMAGUCHI, T., SAMESHIMA, Y., GOTO, M. & FURUKAWA, K. (2004) Molecular characterization of protein *O*-mannosyltransferase and its involvement in cell-wall synthesis in *Aspergillus nidulans*. *Microbiology,* 150**,** 1973-82.

OKAMOTO, M., YOKO-O, T., UMEMURA, M., NAKAYAMA, K. & JIGAMI, Y. (2006) Glycosylphosphatidylinositol-anchored proteins are required for the

transport of detergent-resistant microdomain-associated membrane proteins Tat2p and Fur4p. *J Biol Chem,* 281**,** 4013-23.

ORLEAN, P. (1990) Dolichol phosphate mannose synthase is required in vivo for glycosyl phosphatidylinositol membrane anchoring, *O* mannosylation, and *N* glycosylation of protein in *Saccharomyces cerevisiae*. *Mol Cell Biol,* 10**,** 5796-805.

PEAT, S., TURVEY, J. R. & DOYLE, D. (1961) The polysaccharides of baker's yeast. Part V. A further study of the mannan. *J Chem Soc***,** 3918–3923.

PILON, M., SCHEKMAN, R. & ROMISCH, K. (1997) Sec61p mediates export of a misfolded secretory protein from the endoplasmic reticulum to the cytosol for degradation. *Embo J,* 16**,** 4540-8.

POPOLO, L. & VAI, M. (1999) The Gas1 glycoprotein, a putative wall polymer cross-linker. *Biochim Biophys Acta,* 1426**,** 385-400.

PROSZYNSKI, T. J., SIMONS, K. & BAGNAT, M. (2004) *O*-glycosylation as a sorting determinant for cell surface delivery in yeast. *Mol Biol Cell,* 15**,** 1533-43.

SANDERS, S. L., GENTZSCH, M., TANNER, W. & HERSKOWITZ, I. (1999) *O*-Glycosylation of Axl2/Bud10p by Pmt4p is required for its stability, localization, and function in daughter cells. *J Cell Biol,* 145**,** 1177-88.

SCHACHTER, H. (1991) The 'yellow brick road' to branched complex *N*-glycans. *Glycobiology,* 1**,** 453-61.

SIKORSKI, R. S. & HIETER, P. (1989) A system of shuttle vectors and yeast host strains designed for efficient manipulation of DNA in *Saccharomyces cerevisiae*. *Genetics,* 122**,** 19-27.

SITIA, R. & BRAAKMAN, I. (2003) Quality control in the endoplasmic reticulum protein factory. *Nature,* 426**,** 891-4.

SPEAR, E. D. & NG, D. T. (2005) Single, context-specific glycans can target misfolded glycoproteins for ER-associated degradation. *J Cell Biol,* 169**,** 73-82.

SPIRO, R. G. (2002) Protein glycosylation: nature, distribution, enzymatic formation, and disease implications of glycopeptide bonds. *Glycobiology,* 12**,** 43R-56R.

STRAHL-BOLSINGER, S., IMMERVOLL, T., DEUTZMANN, R. & TANNER, W. (1993) *PMT1*, the gene for a key enzyme of protein *O*-glycosylation in *Saccharomyces cerevisiae*. *Proc Natl Acad Sci U S A,* 90**,** 8164-8.

STRAHL-BOLSINGER, S., GENTZSCH, M. & TANNER, W. (1999) Protein *O*-

mannosylation. *Biochim Biophys Acta,* 1426**,** 297-307.

SUTTON, A., IMMANUEL, D. & ARNDT, K. T. (1991) The *SIT4* protein phosphatase functions in late G1 for progression into S phase. *Mol Cell Biol,* 11**,** 2133-48.

TANIGUCHI, N. (2003) [Importance of sugar chain functions and their characterization]. *Tanpakushitsu Kakusan Koso,* 48**,** 901-9.

TAXIS, C., VOGEL, F. & WOLF, D. H. (2002) ER-golgi traffic is a prerequisite for efficient ER degradation. *Mol Biol Cell,* 13**,** 1806-18.

TRIMBLE, R. B. & ATKINSON, P. H. (1986) Structure of yeast external invertase Man8-14GlcNAc processing intermediates by 500-megahertz 1H NMR spectroscopy. *J Biol Chem,* 261**,** 9815-24.

VAI, M., GATTI, E., LACANA, E., POPOLO, L. & ALBERGHINA, L. (1991) Isolation and deduced amino acid sequence of the gene encoding gp115, a yeast glycophospholipid-anchored protein containing a serine-rich region. *J Biol Chem,* 266**,** 12242-8.

VANDERVEN, B. C., HARDER, J. D., CRICK, D. C. & BELISLE, J. T. (2005) Export-mediated assembly of mycobacterial glycoproteins parallels eukaryotic pathways. *Science,* 309**,** 941-3.

VASHIST, S., KIM, W., BELDEN, W. J., SPEAR, E. D., BARLOWE, C. & NG, D. T. (2001) Distinct retrieval and retention mechanisms are required for the quality control of endoplasmic reticulum protein folding. *J Cell Biol,* 155**,** 355-68.

VASHIST, S. & NG, D. T. (2004) Misfolded proteins are sorted by a sequential checkpoint mechanism of ER quality control. *J Cell Biol,* 165**,** 41-52.

WEBER, Y., PRILL, S. K. & ERNST, J. F. (2004) Pmt-mediated *O* mannosylation stabilizes an essential component of the secretory apparatus, Sec20p, in *Candida albicans*. *Eukaryot Cell,* 3**,** 1164-8.

WILLER, T., AMSELGRUBER, W., DEUTZMANN, R. & STRAHL, S. (2002) Characterization of *POMT2*, a novel member of the *PMT* protein *O*-mannosyltransferase family specifically localized to the acrosome of mammalian spermatids. *Glycobiology,* 12**,** 771-83.

WILLER, T., VALERO, M. C., TANNER, W., CRUCES, J. & STRAHL, S. (2003) *O*-mannosyl glycans: from yeast to novel associations with human disease. *Curr Opin Struct Biol,* 13**,** 621-30.

XU, X., AZAKAMI, H. & KATO, A. (2004) P-domain and lectin site are involved in

the chaperone function of *Saccharomyces cerevisiae* calnexin homologue. *FEBS Lett,* 570**,** 155-60.

YAN, A. & LENNARZ, W. J. (2005) Two oligosaccharyl transferase complexes exist in yeast and associate with two different translocons. *Glycobiology,* 15**,** 1407-15.

YAN, Q. & LENNARZ, W. J. (2002) Studies on the function of oligosaccharyl transferase subunits. Stt3p is directly involved in the glycosylation process. *J Biol Chem,* 277**,** 47692-700.

YOSHIDA, A., KOBAYASHI, K., MANYA, H., TANIGUCHI, K., KANO, H., MIZUNO, M., INAZU, T., MITSUHASHI, H., TAKAHASHI, S., TAKEUCHI, M., HERRMANN, R., STRAUB, V., TALIM, B., VOIT, T., TOPALOGLU, H., TODA, T. & ENDO, T. (2001) Muscular dystrophy and neuronal migration disorder caused by mutations in a glycosyltransferase, POMGnT1. *Dev Cell,* 1**,** 717-24.

YUEN, C. T., CHAI, W., LOVELESS, R. W., LAWSON, A. M., MARGOLIS, R. U. & FEIZI, T. (1997) Brain contains HNK-1 immunoreactive *O*-glycans of the sulfoglucuronyl lactosamine series that terminate in 2-linked or 2,6-linked hexose (mannose). *J Biol Chem,* 272**,** 8924-31.

FIGURES AND TABLES

Table I. Plasmid used in this study

Plasmid	Description	Source
pSM70	HA-tagged *KHN* driven by *PRC1* promoter, *CEN/ARS, URA3*	Vashist *et al*., 2001
pHI101	HA-tagged *GAS1*, *CEN/ARS*, *URA3*	This study
pHI102	HA-tagged *gas1-871,873*, *CEN/ARS, URA3*	This study
pHI118	HA-tagged sol-*GAS1*, *CEN/ARS, URA3*	This study
pHI119	HA-tagged sol-*gas1-871,873, CEN/ARS, URA3*	This study
pMF848	HA-tagged *prc1-1, CEN/ARS, URA3*	This study

Table II. Yeast strains used in this study

Strain	Harboring plasmid	Genotype	Source
W303-1A	–	*MAT***a** *leu2-3,112 his3-11 ade2-1 ura3-1 trp1-1 can1-100*	Sutton *et al*., 1991
YJY1	–	*MAT***a** *his3*Δ*1 leu2*Δ*0 met15*Δ*0 ura3*Δ*0* (S288C background)	Lab strain
BY4741	–	*MAT***a** *his3*Δ*1 leu2*Δ*0 met15*Δ*0 ura3*Δ*0*	ATCC
BY4742	–	*MAT*α *his3*Δ*1 leu2*Δ*0 lys2*Δ*0 ura3*Δ*0*	ATCC
SSY18	–	*MAT***a** *ktr1*Δ*::hisG kre2*Δ*::hisG ktr3*Δ*::hisG* W303	Lab strain
YME1305	pHI102	*MAT***a** YJY1	This study
*pmt1*Δ	–	*MAT***a** *pmt1*Δ*::kanMX6* BY4741	SDP
*pmt2*Δ	–	*MAT***a** *pmt2*Δ*::kanMX6* BY4741	SDP
*pmt3*Δ	–	*MAT***a** *pmt3*Δ*::kanMX6* BY4741	SDP
*pmt4*Δ	–	*MAT***a** *pmt4*Δ*::His3MX6* YJY1	This study
*pmt5*Δ	–	*MAT***a** *pmt5*Δ*::kanMX6* BY4741	SDP
*pmt6*Δ	–	*MAT***a** *pmt6*Δ*::kanMX6* BY4741	SDP
YME318	pHI101	*MAT***a** SSY18	This study
YME319	pHI102	*MAT***a** SSY18	This study
YME335	pHI118	*MAT***a** SSY18	This study
YME336	pHI119	*MAT***a** SSY18	This study
YME1315	pHI102	*MAT***a** *pmt1*Δ*::kanMX6* BY4741	This study
YME1316	pHI102	*MAT***a** *pmt2*Δ*::kanMX6* BY4741	This study
YME1317	pHI102	*MAT***a** *pmt3*Δ*::kanMX6* BY4741	This study
YME1334	pHI102	*MAT***a** *pmt4*Δ*::His3MX6* YJY1	This study
YME1318	pHI102	*MAT***a** *pmt5*Δ*::kanMX6* BY4741	This study
YME1319	pHI102	*MAT***a** *pmt6*Δ*::kanMX6* BY4741	This study
YME1336	pHI102	*MAT***a** *pmt1*Δ*::His3MX6 pmt2*Δ*::kanMX6* BY4741	This study
YME1374	pHI102	*MAT***a** *pmt4*Δ*::His3MX6 pmt6*Δ*::kanMX6* BY4741	This study
YME1384	pHI102	*MAT***a** *pep4*Δ*::His3MX6* BY4741	This study
YME1385	pHI102	*MAT***a** *pep4*Δ*::LEU2 pmt1*Δ*::His3MX6 pmt2*Δ*::kanMX6* BY4741	This study
YME1392	pHI102	*MAT***a** *pep4*Δ*::LEU2 pmt4*Δ*::His3MX6 pmt6*Δ*::kanMX6* BY4741	This study
YME1398	pHI119	*MAT***a** BY4741	This study
YME1399	pHI119	*MAT*α *pep4*Δ*::LEU2* BY4742	This study
YME1400	pHI119	*MAT***a** *pep4*Δ*::LEU2 pmt1*Δ*::His3MX6 pmt2*Δ*::kanMX6* BY4741	This study
YME1421	pMF848	*MAT***a** BY4741	This study
YME1422	pMF848	*MAT*α *pep4*Δ*::LEU2* BY4742	This study
YME1423	pMF848	*MAT***a** *pep4*Δ*::LEU2 pmt1*Δ*::His3MX6 pmt2*Δ*::kanMX6* BY4741	This study
YME1425	pHI119	*MAT***a** BY4741	This study
YME1426	pHI119	*MAT***a** *pmt1*Δ*::kanMX6* BY4741	This study
YME1427	pHI119	*MAT***a** *pmt2*Δ*::kanMX6* BY4741	This study
YME1428	pHI119	*MAT***a** *pmt3*Δ*::kanMX6* BY4741	This study
YME1429	pHI119	*MAT***a** *pmt4*Δ*::His3MX6* YJY1	This study
YME1430	pHI119	*MAT***a** *pmt5*Δ*::kanMX6* BY4741	This study
YME1431	pHI119	*MAT***a** *pmt6*Δ*::kanMX6* BY4741	This study
YME1440	pHI102	*MAT*α *vps38*Δ*::His3MX6 pmt1*Δ*::LEU2 pmt2*Δ*::kanMX6 ura3*Δ*0 lys2*Δ*0*	This study
YME1444	pHI102	*MAT***a** *vps38*Δ*::kanMX6* BY4741	This study
YME1445	pSM70	*MAT***a** BY4741	This study
YME1446	pSM70	*MAT***a** *pmt1*Δ*::His3MX6 pmt2*Δ*::kanMX6* BY4741	This study
YME1447	pSM70	*MAT***a** *pep4*Δ*::LEU2 pmt1*Δ*::His3MX6 pmt2*Δ*::kanMX6* BY4741	This study

SDP, *Saccharomyces* Deletion Project (http://www-deletion.stanford.edu/YDPM/index.html); ATCC, American Type Culture Collection; Lab strain, laboratory strain.

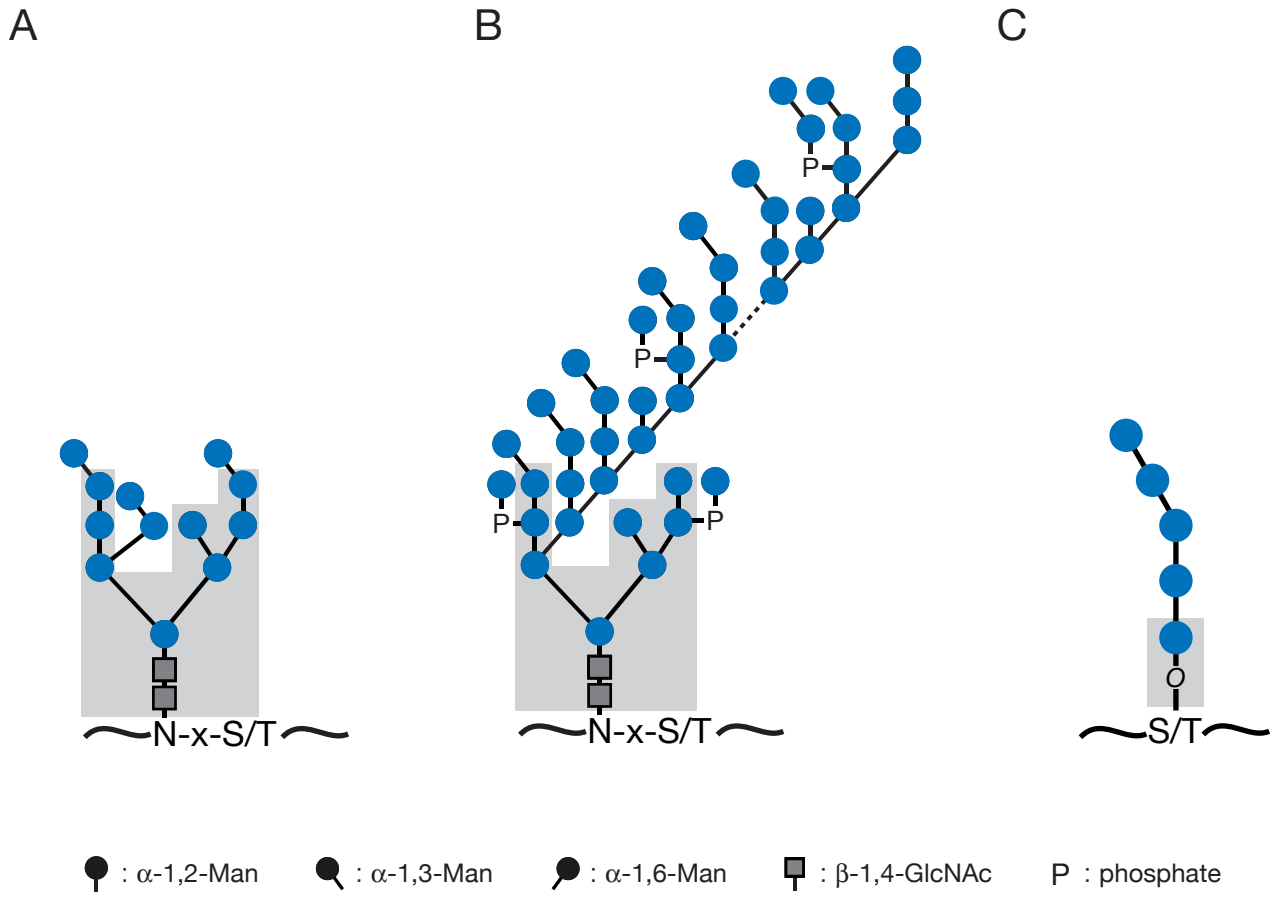

Figure 1. Structure of *N* and *O*- linked sugar chain in *S. cerevisiae*

(A) The core-type structure of *N*-glycan. (B) The mannan structure of *N*-glycan. The side chain backbone consists of approximatly 50, and the entire structure, of over 200 mannose residues. (C) The structure of *O*-glycan. Gray boxes indicat the structures that are synthesized in the ER

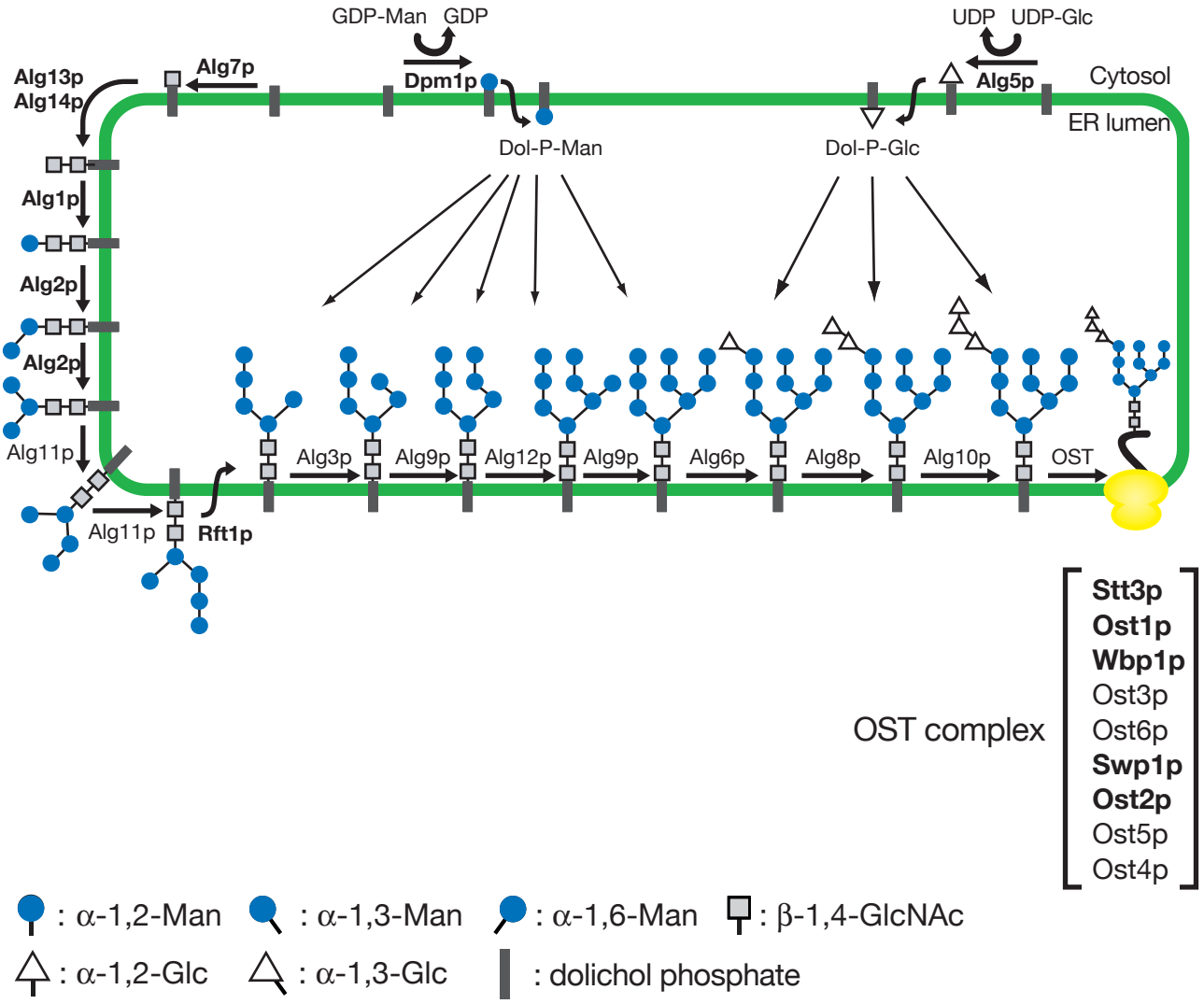

Figure 2. The biosynthesis pathway of *N*-glycan core structure ($Glc_3Man_9GlcNAc_2$) in the ER

The identified *ALG* gene products for the respective glycosylation reactions are indicated (essential genes are indicated in boldface). Synthesis reaction starts at the cytoplasmic face with UDP-GlcNAc and GDP-Man as glycosyl donors. The dolicholphosphate-linked $Man_5GlcNAc_2$ is then transferred to the luminal side with the help of Rft1p and elongated to the full-length lipid-linked oligosaccharide ($Glc_3Man_9GlcNAc_2$-PP-Dol) by using Dol-P-Man and Dol-P-Glc. The oligosaccharide is subsequently transferred to the asparagine residues within the consensus sequence Asn-X-Ser/Thr of nascent secretory proteins. This reaction is catalyzed by the oligosaccharyl transferase (OST) complex. Adapted from Lehle *et al.*, 2006.

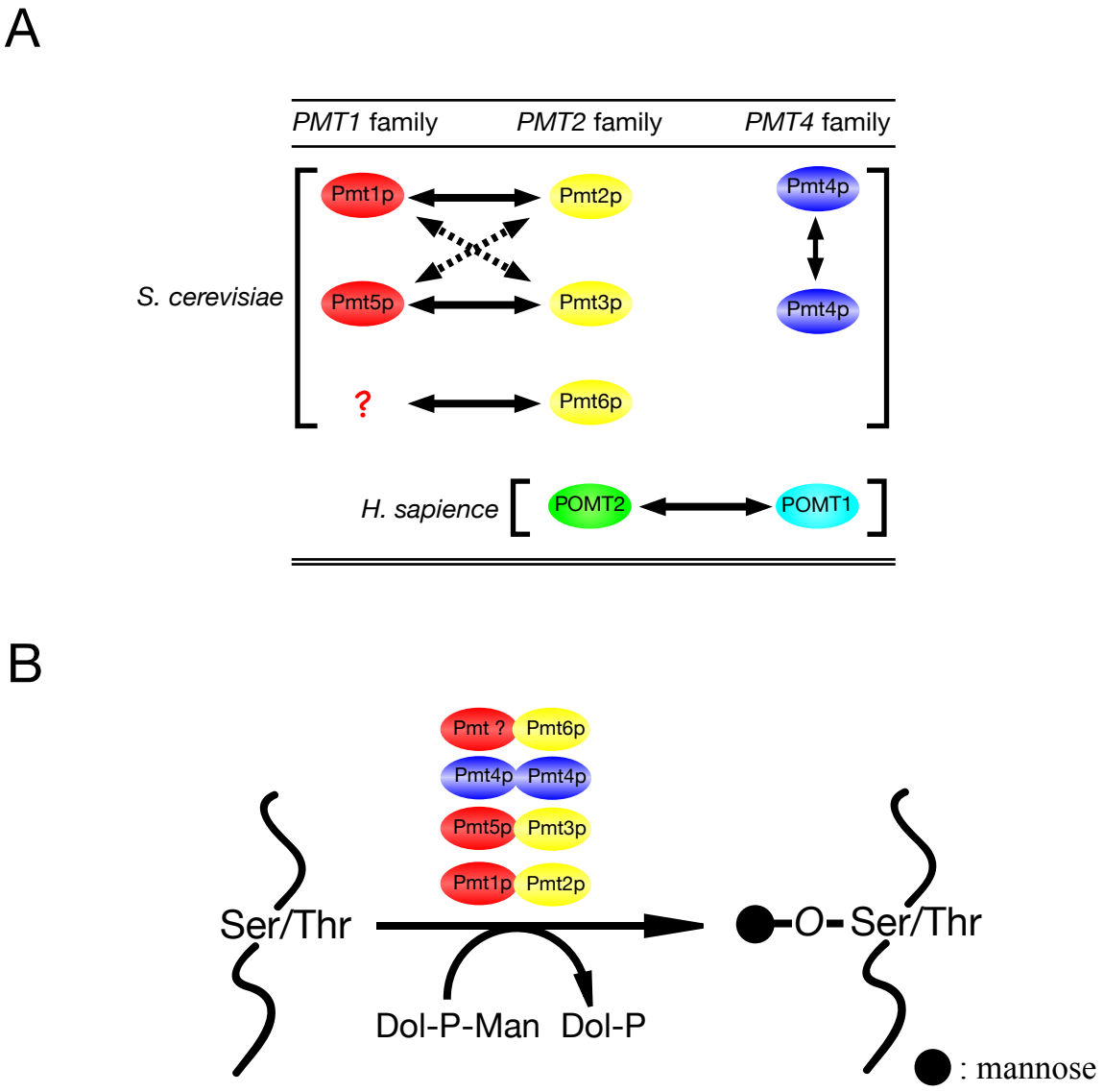

Figure 3. Protein–Protein interaction of *PMT* families in *S. cerevisiae*

(A) Pmts (Pmt1p–Pmt6p) is classified into three families, *PMT1*, *PMT2*, and *PMT4* families, by their similality. Pmt1p and Pmt2p, Pmt5p and Pmt3p form heterocomplexes, whereas Pmt4p forms homocomplex as indicated solid lines. These complexes are essential for mannosyltransferase activity of Pmt proteins. when one of the principal partners is absent, Pmt1p can interact with Pmt3p, and Pmt5p with Pmt2p, respectively (broken line). Whereas, Human protein *O*-mannosyltransferases (POMT1 and POMT2) also form heterocomplex (solid line) which is also essential for their mannosyltransferase activity. (B) Each Pmt subfamily recognizes different acceptor substrates and mannose is transferred to Ser/Thr residues of various proteins using dolichol-phosphate mannose as a mannosyl doner.

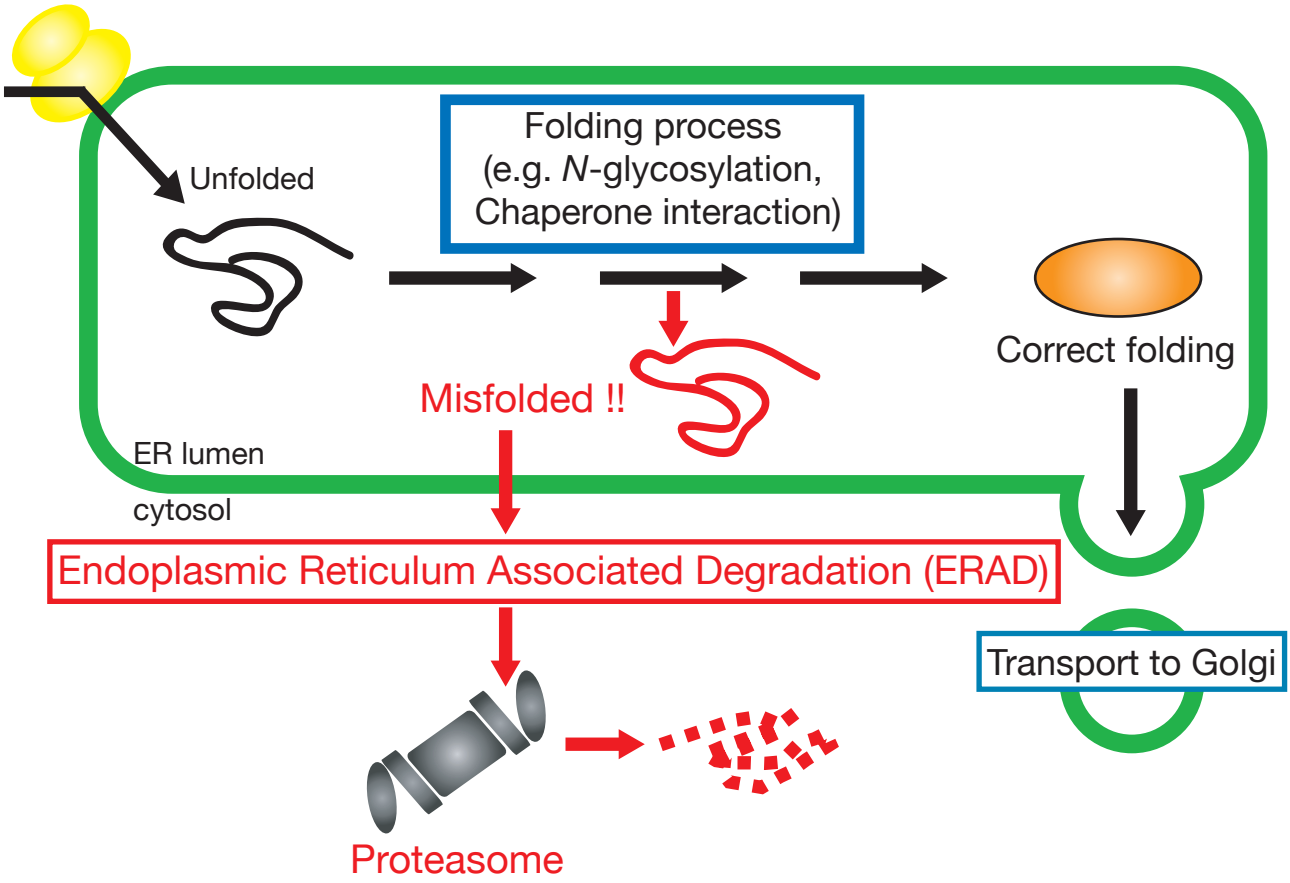

Figure 4. Protein folding and quality control in the ER

Folding of proteins are carried out in the ER. Correctly folded proteins are transported from the ER to the Gogi, whereas misfolded proteins are recognized and degraded by the 26S proteasome after retrotranslocation into the cytosol and ubiquitination. This process is called by ER-associated degradation (ERAD).

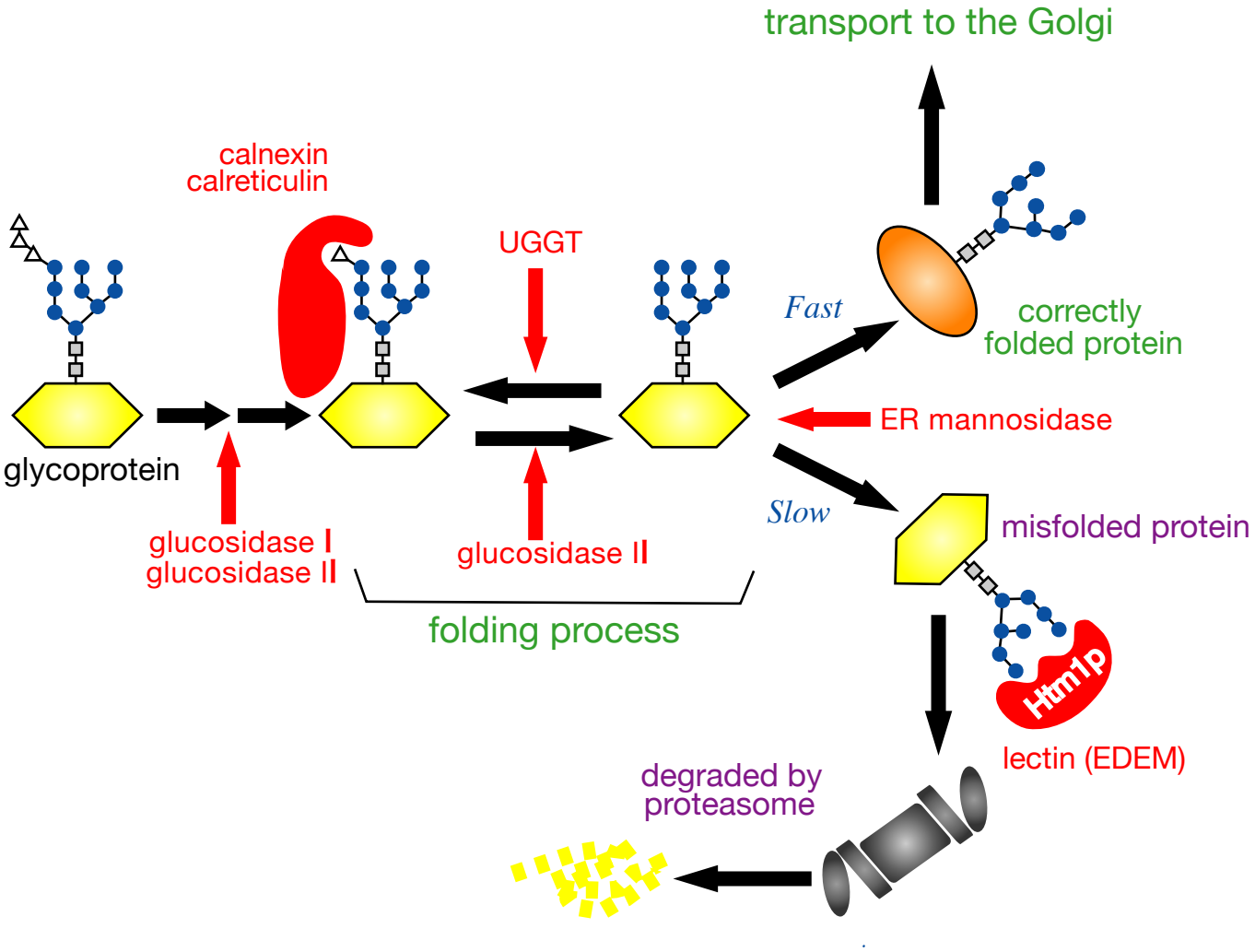

Figure 5. Involvement of *N*-glycosylation in the ER quality control

After addition of core glycan ($Glc_3Man_9GlcNAc_9$) to a nascent polypeptide chain by oligosacchride transferase, the outermost of the three glucose residues is removed by glucosidase I. Soon thereafter, glucosidase II removes the middle glucose. Via the monoglucosylated core glycans thus generated, the glycoprotein binds to monoglucosylated glycans binding chaperons, calnexin and calreticulin. These sequester the nacent or newly synthesized chains and expose them to PDI, a thiol-disulfide oxidoreducase that provides assistance during disulfide bond formation. When glucosidase II remove the remaining glucose, the glucoprotein dissociates from calnexin and calreticulin. The protein now encounters one of three possible fates. If properly folded, mannose residue is trimmed by ER mannosidase I rapidly and the protein leaves the ER. In mammalian systems, if it is in completely folded, UDP-Glc:glycoprotein glucosyltransferase (UGGT) uses UDP-glucose transported by a UDP-glucose/UMP exchanger from the cytosol to reglucosylate the $Man_9GlcNAc_2$ glycan located in improperly folded region. While, there is no UGGT activity in *S. cerevisiae*. Through these glycans, the glycoprotein rebind to calnexin and calreticulin. The third fate is ERAD after retrotranslocation of the misfolded glycoprotein to the ER most likely through the translocon complex. ERAD of glycoproteins occures when they have stayed in the ER lumen for some time and when they are recognizsed by a putative lectin (EDEM) because they have lost a mannose through the action of ER mannosidase I. Triangles are glucose residues. Blue circles are mannose, and Grey squares are GlcNAc, respectively.

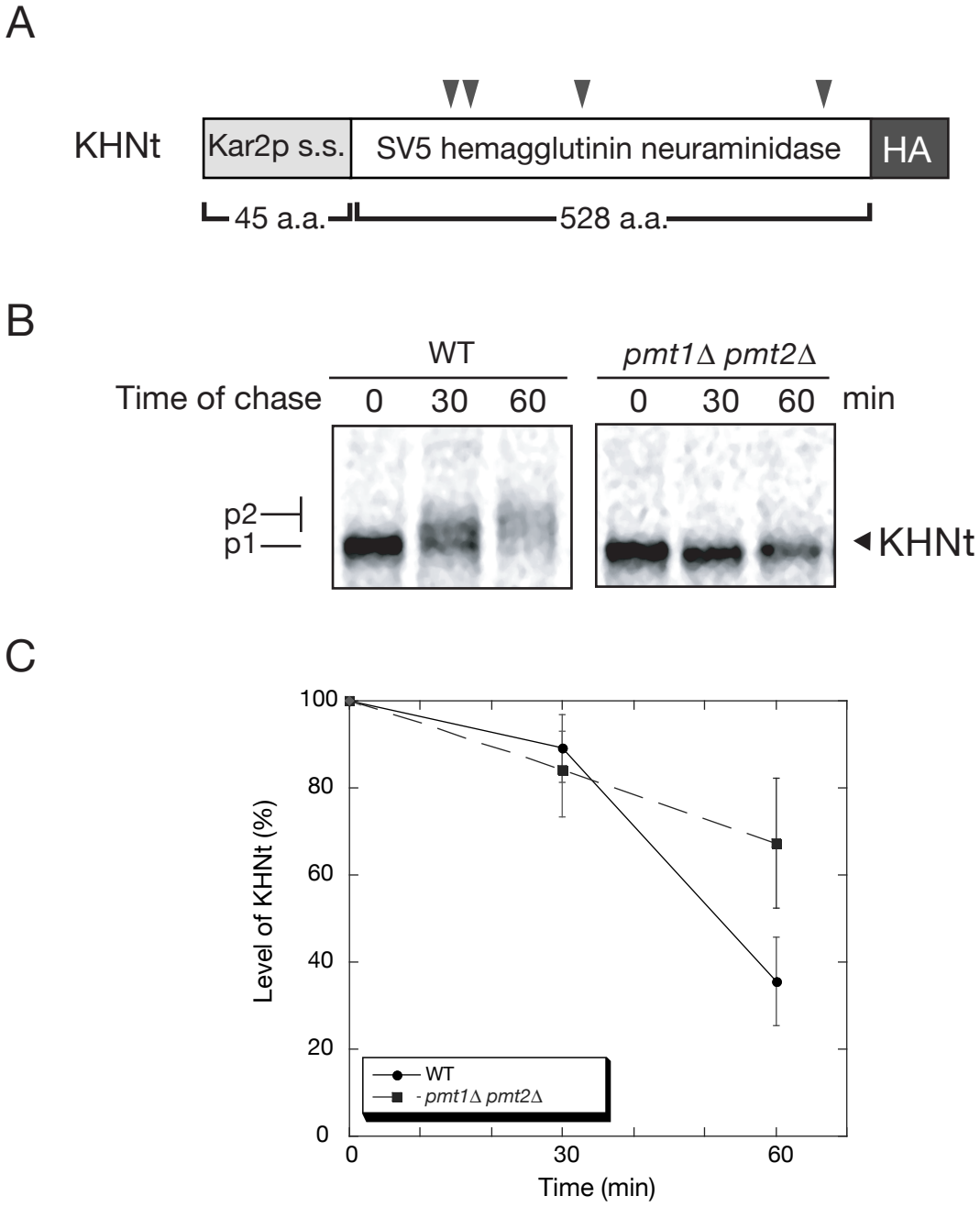

Figure 6. The rate of degradation of KHNt is reduced in *pmt1*Δ *pmt2*Δ cells.

(A) Schematic construction of HA-tagged KHN (KHNt). KHN is fusion protein of yeast Kar2p segnal sequcence and SV5 hemagglutinin neuraminidase (HN). 3xHA tag was inserted into C-terminal of KHN. Vertical arrow heads indicate potential *N*-glycosylation site (Asn-X-Ser/Thr).
(B) KHNt expressed in wild-type (YME1445) and *pmt1*Δ *pmt2*Δ (YME1446) cells were pulse-labeled with [^{35}S]-cysteine/methionine for 10 min and chase for the indicated amount of time. KHNt was recovered from cell lysete by immunoprecicitaiton using anti-HA agarose beads. The samples were separeted by SDS-PAGE and detected autoradiography. p1 and p2 refer to ER form and Golgi form (*N* and *O*-linked sugar chain elongate form) of KHNt, respectively. (C) The percentages of KHNt bands relative to the band of time point 0. Data points and error bars indicate means values ±SD from three independent experiments.

Figure 7. KHNt forms severe aggregates in *pmt1*Δ *pmt2*Δ cells

(A) Whole-cell lysates were prepared from KHNt expressing wild-type (YME1445) and *pmt1*Δ *pmt2*Δ (YME1446) cells. Cell lysates (300 μg of protein) were subjected to 5–50% linear sucrose density gradient centrifugation. Fractions were collected and analyzed by SDS-PAGE, followed by Immunoblotting using an anti-HA antibody (1:4000) and HRP-conjugated anti-mouse IgG antibody (1:4000) (see "**MATERIALS AND METHODS**"). (B) Relative amounts of KHNt in each fraction were quantified. Vertical arrowheads indicate the position of ferritin (440 kDa), catalase (232 kDa), aldolase (158 kDa), and ovalbumin (43 kDa), respectively. (C) Membranes of YME1445 and YME1446 strains were solubilized in 1% TritonX-100 and separated into pellet and supernatant fractions by centrifugation (see "Materials and methods"). Total (T), detergent-soluble (S), and detergent-insoluble pellet (P) fractions were resolved by SDS-PAGE, followed by immunoblot using an anti-HA antibody (1:10000) and HRP-conjugated anti-mouse IgG antibody (1:10000). The extent of membrane solubilization was determined by immunoblot of Dpm1p using anti-Dpm1p antibody (1:5000) followed by HRP-conjugated anti-mouse IgG antibody (1:10000). p1 and p2 refer to ER form and Golgi form (*N* and *O*-linked sugar chain elongate form) of KHNt, respectively, respectively.

A

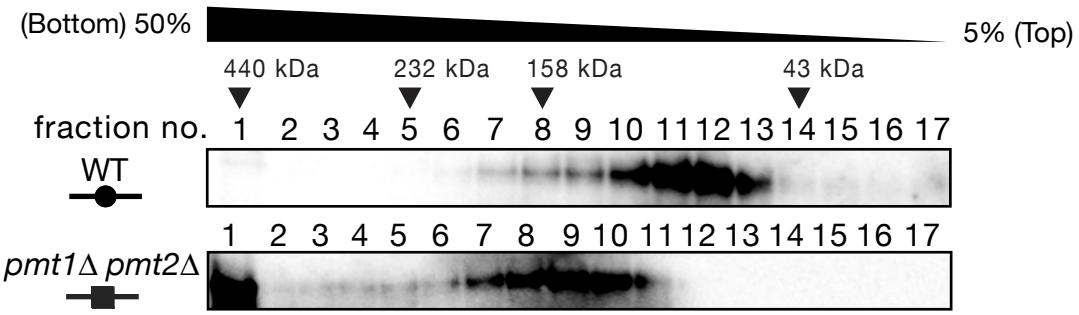
(Bottom) 50%
5% (Top)
440 kDa
232 kDa
158 kDa
43 kDa
fraction no. 1 2 3 4 5 6 7 8 9 10 11 12 13 14 15 16 17
WT
1 2 3 4 5 6 7 8 9 10 11 12 13 14 15 16 17
pmt1Δ pmt2Δ

B

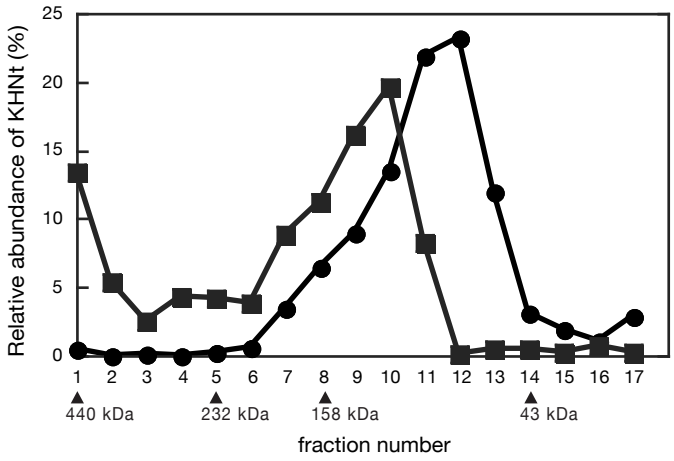
Relative abundance of KHNt (%)
25
20
15
10
5
0
1 2 3 4 5 6 7 8 9 10 11 12 13 14 15 16 17
440 kDa
232 kDa
158 kDa
43 kDa
fraction number

C

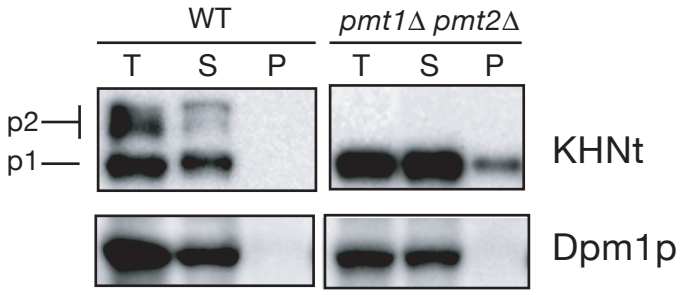
WT
pmt1Δ pmt2Δ
T S P T S P
p2
p1
KHNt
Dpm1p

Figure 8. Model for the function of *O*-mannosylation, executed by Pmt1p and Pmt2p, to KHNt in ERQC systems

In wild-type cells, excessively *O*-mannosylated KHNt can exit the ER and target to ERAD via ERAD-L pathway and is degraded by 26S proteasome (A). on the other hand, underglycosylated KHNt, due to the defect of Pmt1p and Pmt2p, forms severe aggregate and is degraded vacuole proteases dependently after sending to the vacuole via Golgi apparatus (B). Taken together, it is essential for the *O*-mannosylation that is executed by Pmt1p and Pmt2p to alleviate seviere aggregation of KHNt.

A Degradation of KHNt (wild-type cell)

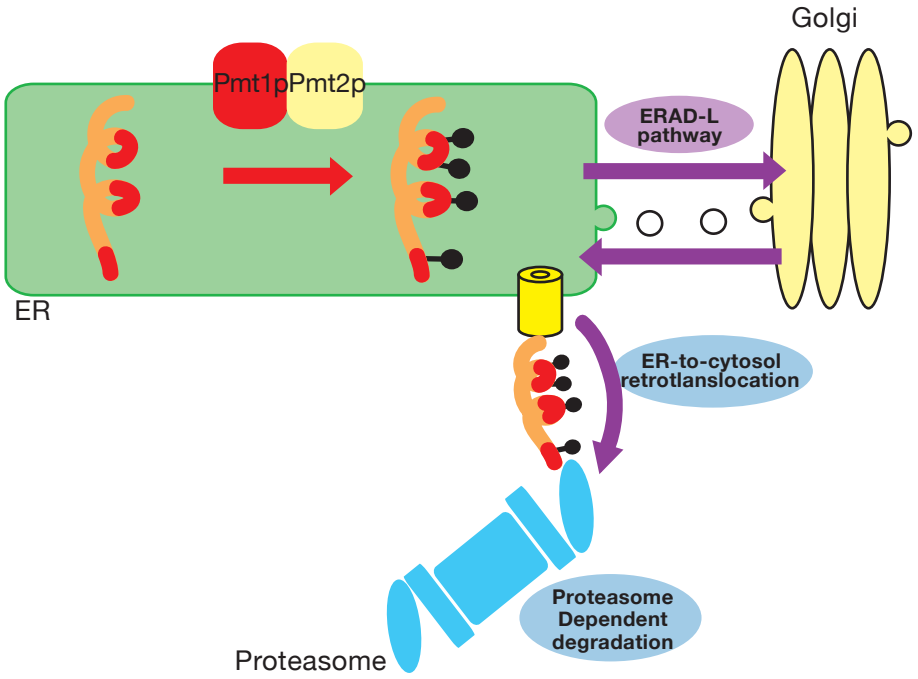

B Degradation of KHNt (*pmt1*Δ *pmt2*Δ cell)

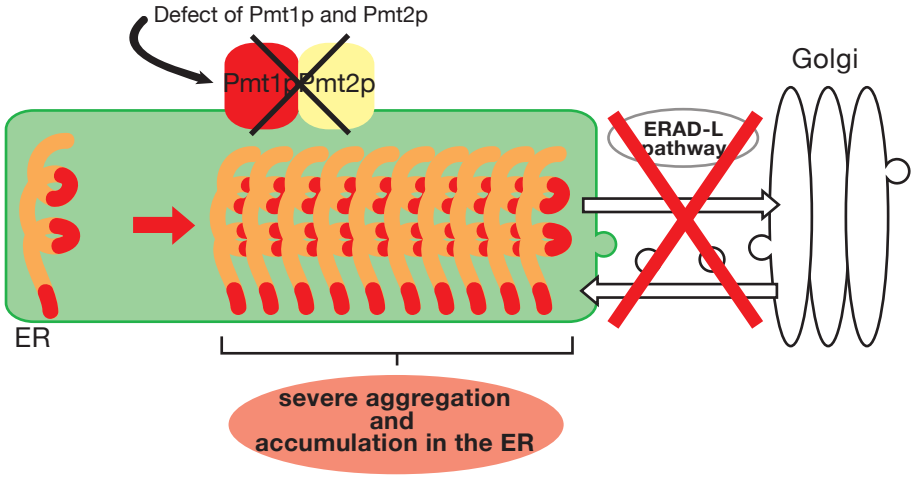

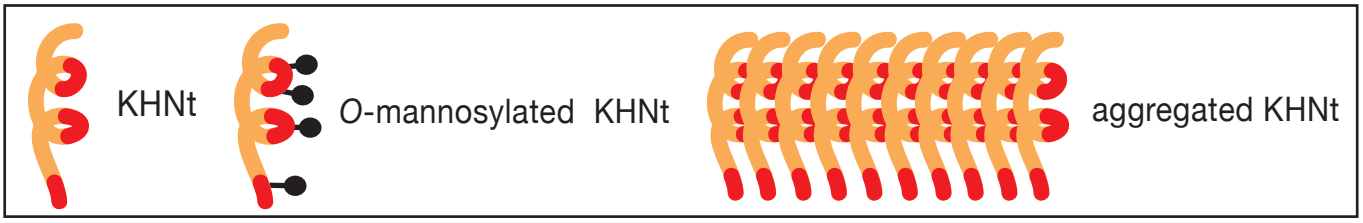

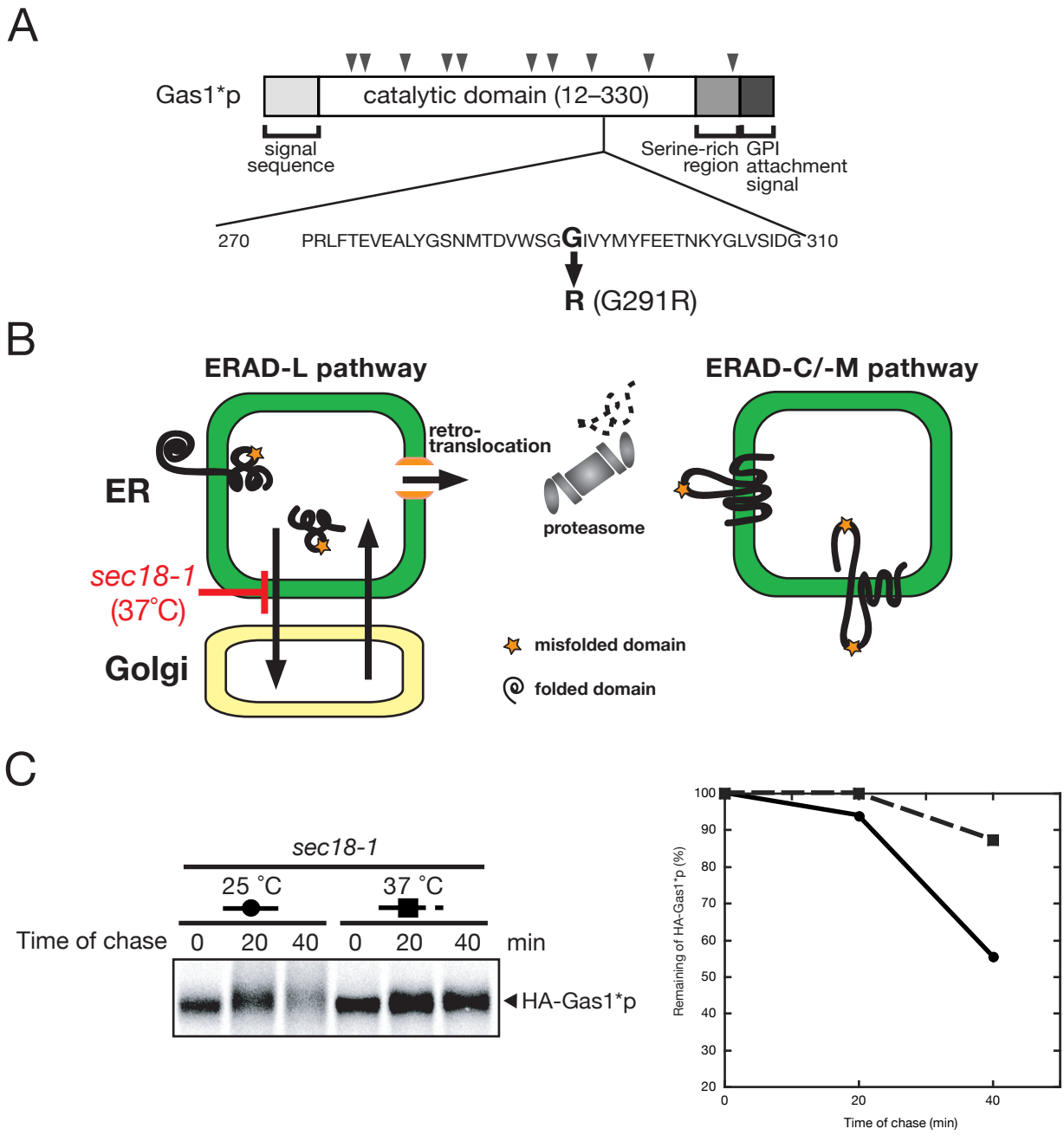

Figure 9. construction of model misfolded protein, Gas1*p

(A) The schematic 1st stracture of Gas1*p, including the sequences of the mutation point (G291R). Vertical arrow heads indicate potential *N*-glycosylation sites (Asn-X-Ser/Thr). (B) Two distinct ERAD pathways are drawn. The ERAD-L pathway system monitors the fold state of lumenal domains, and degradation of ERAD-L substrates to require ER-to-Golgi transport. ERAD-C pathway monitors the folded state of cytosolic domains. ERAD substrates with misfolded domains on both sides of the membrane are degraded by ERAD-C pathway. *sec18-1* mutant defect of ER-to-golgi transport at non-permissing temperature (37˚C) (C) The degradation rate of HA-Gas1*p was mesured in *sec18-1* mutant cells using pulse-chase experiment at non-permissing temperature (25˚C) and permissing temperature (37˚C). Right graph indicates quantified amount of Gas1*p protein as discribed in Figure 6.

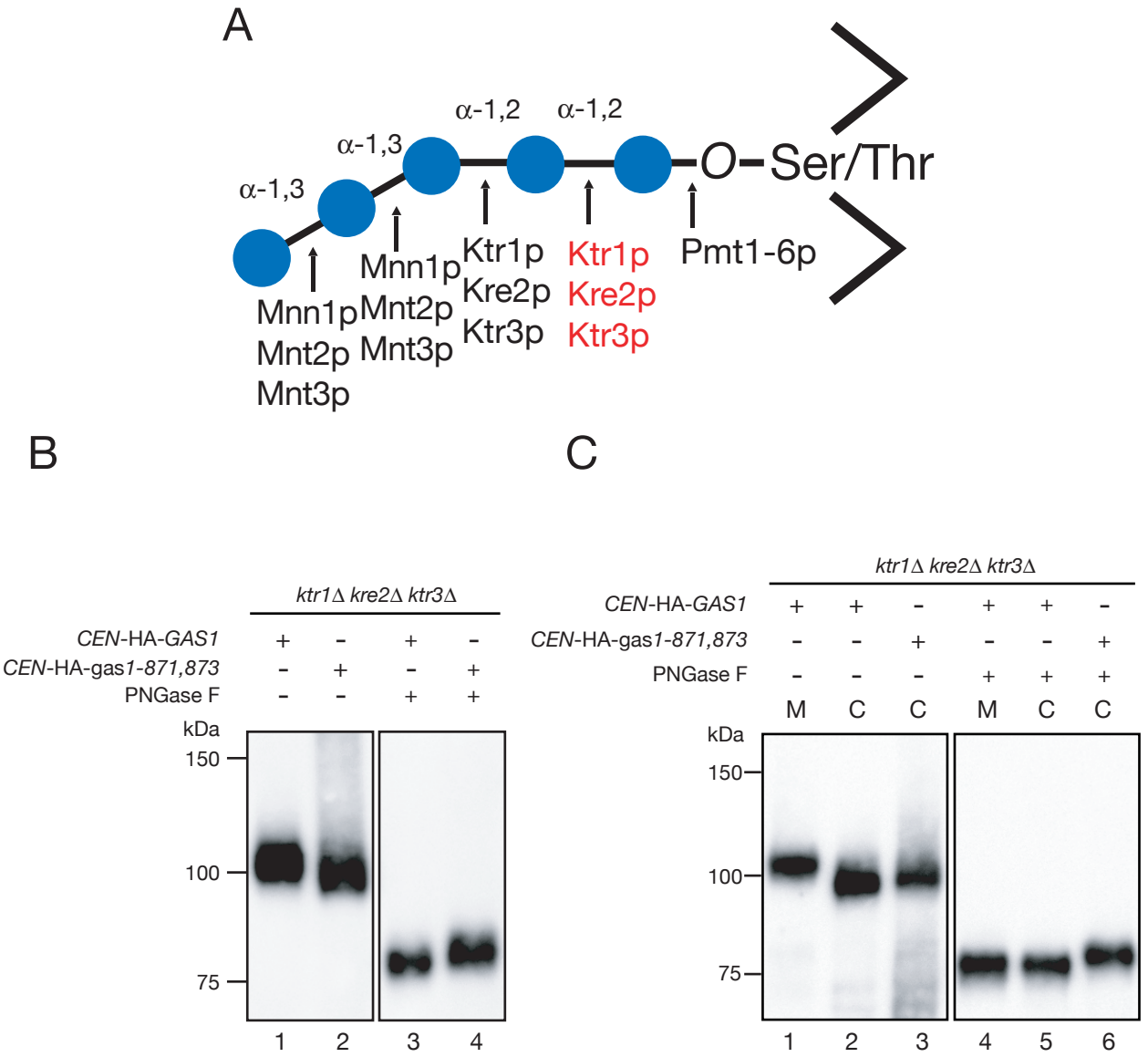

Figure 10. The misfolded proteins HA-Gas1*p and HA-sol-Gas1*p contain more *O*-mannosylated residues than correctly folded Gas1p.

(A) structure of *O*-linked sugar chains in S. cerevisiae. Pmt family adds the first mannose on Ser/Thr residues of proteins in the ER. Ktr1p, Kre2p, and Ktr3p participate in the addition of the second mannose in Golgi apparatus.
(B) 1.0 OD_{600} units of *ktr1*Δ *kre2*Δ *ktr3*Δ cells expressed in HA-Gas1p (YME318) and 4.0 OD_{600} units of that in HA-Gas1*p (YME319) were collected and washed with ice cold water. Whole-cell extracts were prepared as described in "Materials and methods". The same volumes (5 µl) of cell extract were treated with (+) or without (–) PNGase F and denatured with the sample buffer. These samples were separated by SDS-PAGE and visualized by Immunoblotting using anti-HA antibody.
(C) Immunoblot analyses of *ktr1*Δ *kre2*Δ *ktr3*Δ cells expressing HA-sol-Gas1p (YME335) and HA-sol-Gas1*p (YME336). We prepared 1.0 OD_{600} unit of YME335 cells, 4.0 OD_{600} unit of YME336 cells, and 1ml of 5-fold enriched culture medium, in which YME335 cells were grown, and 5 µl of each sample was analyzed. M and C refer to culture medium and cell extract, respectively.

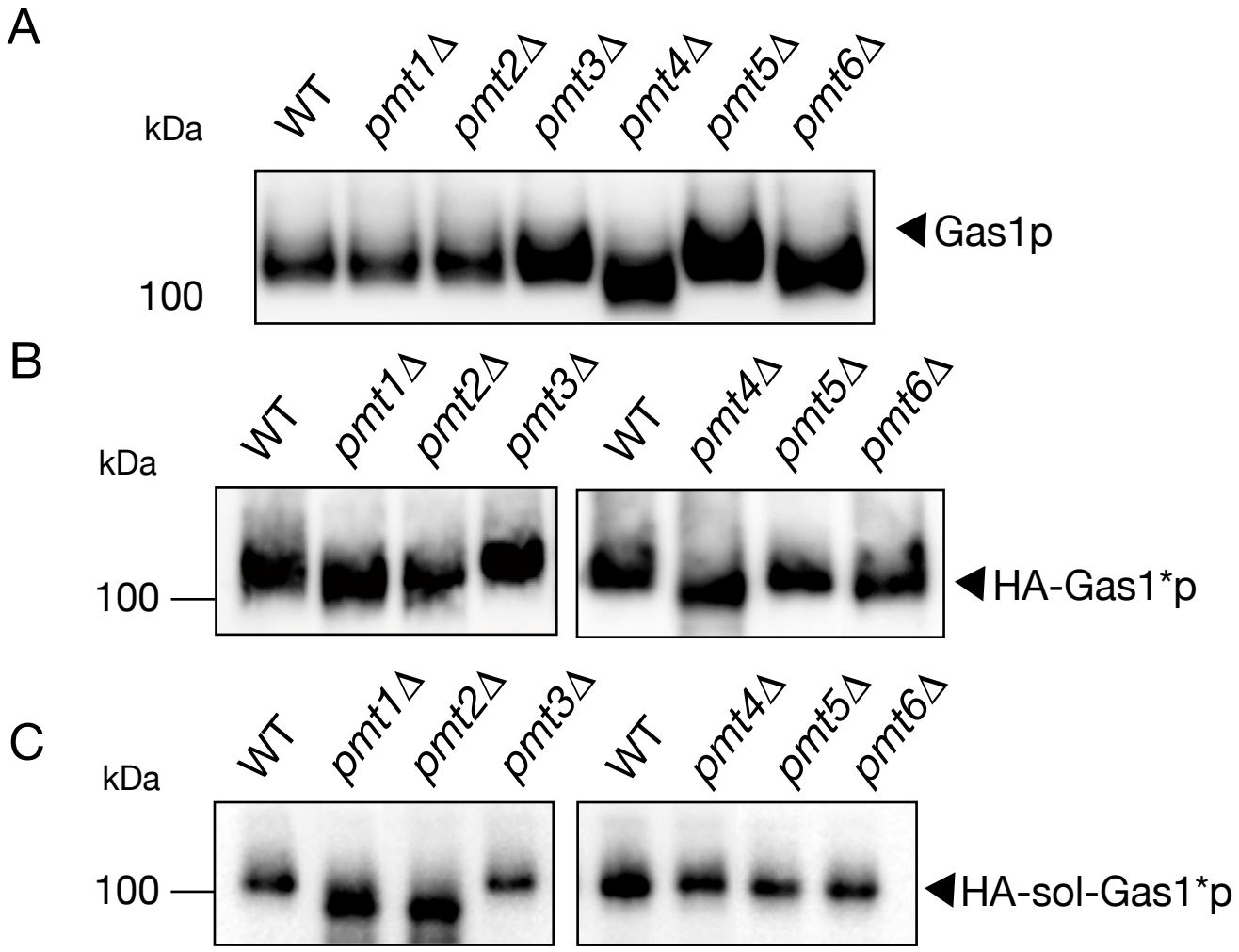

Figure 11. In addition to Pmt4p and Pmt6p, Pmt1p and Pmt2p are responsible for *O*-mannosylation of HA-Gas1*p but not of correctly folded Gas1p.

Whole-cell extracts were prepared from 5.0 OD_{600} units of log-phase cultivated cells. (A) Gas1p extracts (10 µl) from wild-type cells (WT; YJY1) and *pmt1*Δ-*pmt6*Δ mutant cells were denatured with sample buffer and subjected to SDS-PAGE, followed by Immunoblotting with anti-Gas1p antiserum. (B) Immunoblot analysis of HA-Gas1*p expressed in wild-type (YME1305) and *pmt1*Δ (YME1315), *pmt2*Δ (YME1316), *pmt3*Δ (YME1317), *pmt4*Δ (YME1334), *pmt5*Δ (YME1318), and *pmt6*Δ (YME1319) mutant cells. These samples were prepared as described in (A) and detected with an anti-HA antibody. (C) The samples of wild-type (YME1425) and *pmt1*Δ-*pmt6*Δ (YME1426-YME1431) cells expressing HA-sol-Gas1*p were prepared as described in (A) and analyzed with an anti-HA antibody.

Figure 12. HA-Gas1*p expressed in *pmt1*Δ *pmt2*Δ double-mutant cells is degraded in the vacuole.

(A, C) HA-Gas1*p expressed in wild-type (YME1305), *pmt1*Δ *pmt2*Δ (YME1336), *pmt4*Δ *pmt6*Δ (YME1374), *pep4*Δ (YME1384), *pep4*Δ *pmt1*Δ *pmt2*Δ (YME1385), and *pep4*Δ *pmt4*Δ *pmt6*Δ (YME1392) cells were pulse-labeled with [^{35}S]-cysteine/methionine for 10 min and chased for the indicated amounts of time. HA-Gas1*p was recovered from cell lysates by immunoprecipitation using anti-HA agarose beads and treated with PNGase F for 3 h at 37°C. The samples were separated by SDS-PAGE and detected by autoradiography. (B, D) The percentages of HA-Gas1*p bands relative to the band of time point 0. Error bars indicate mean values ± SD from three independent experiments.

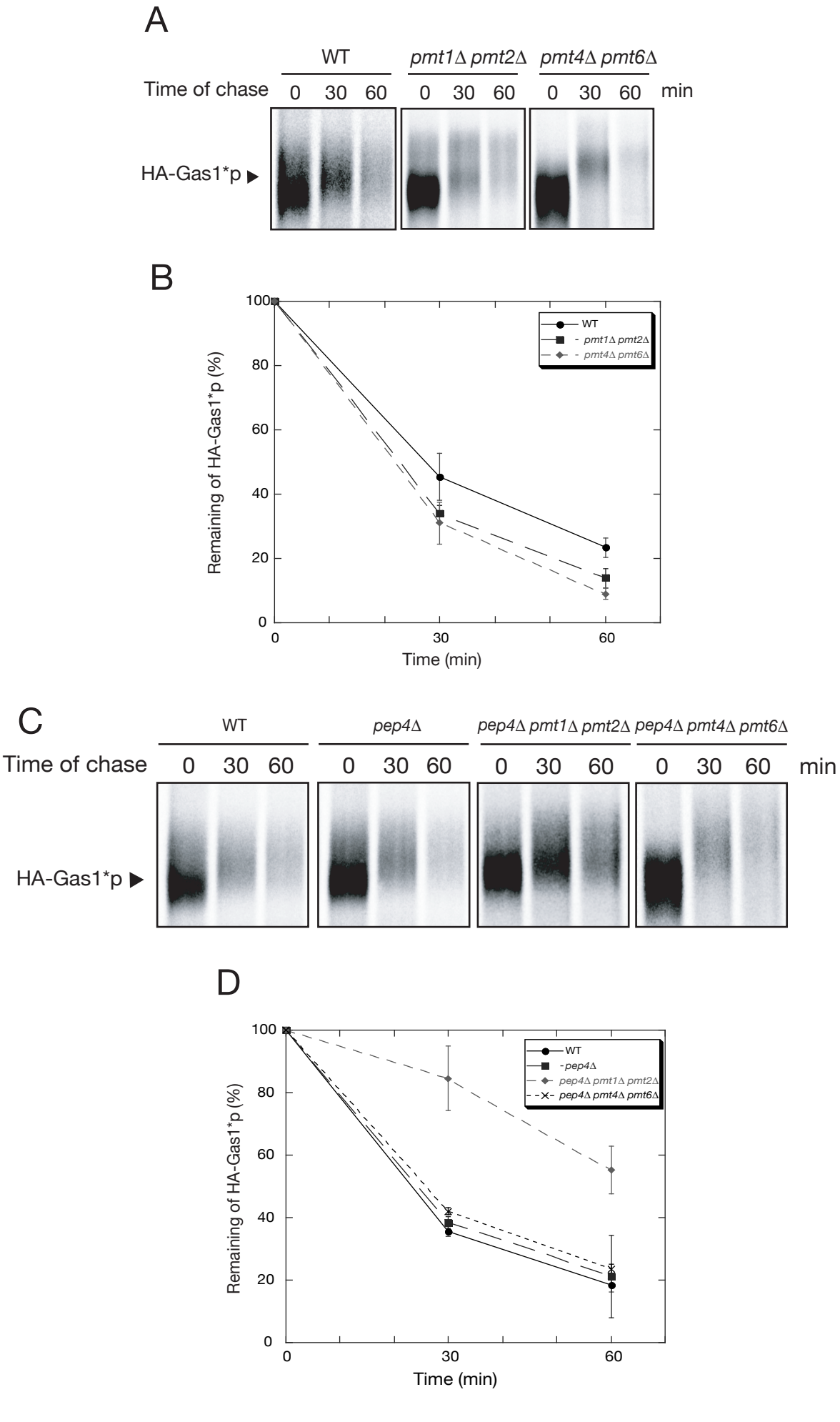
A
WT
pmt1Δ pmt2Δ
pmt4Δ pmt6Δ
Time of chase
0 30 60 0 30 60 0 30 60 min
HA-Gas1*p
B
Remaining of HA-Gas1*p (%)
Time (min)
WT
pmt1Δ pmt2Δ
pmt4Δ pmt6Δ
C
WT
pep4Δ
pep4Δ pmt1Δ pmt2Δ
pep4Δ pmt4Δ pmt6Δ
Time of chase
0 30 60 0 30 60 0 30 60 0 30 60 min
HA-Gas1*p
D
Remaining of HA-Gas1*p (%)
Time (min)
WT
pep4Δ
pep4Δ pmt1Δ pmt2Δ
pep4Δ pmt4Δ pmt6Δ

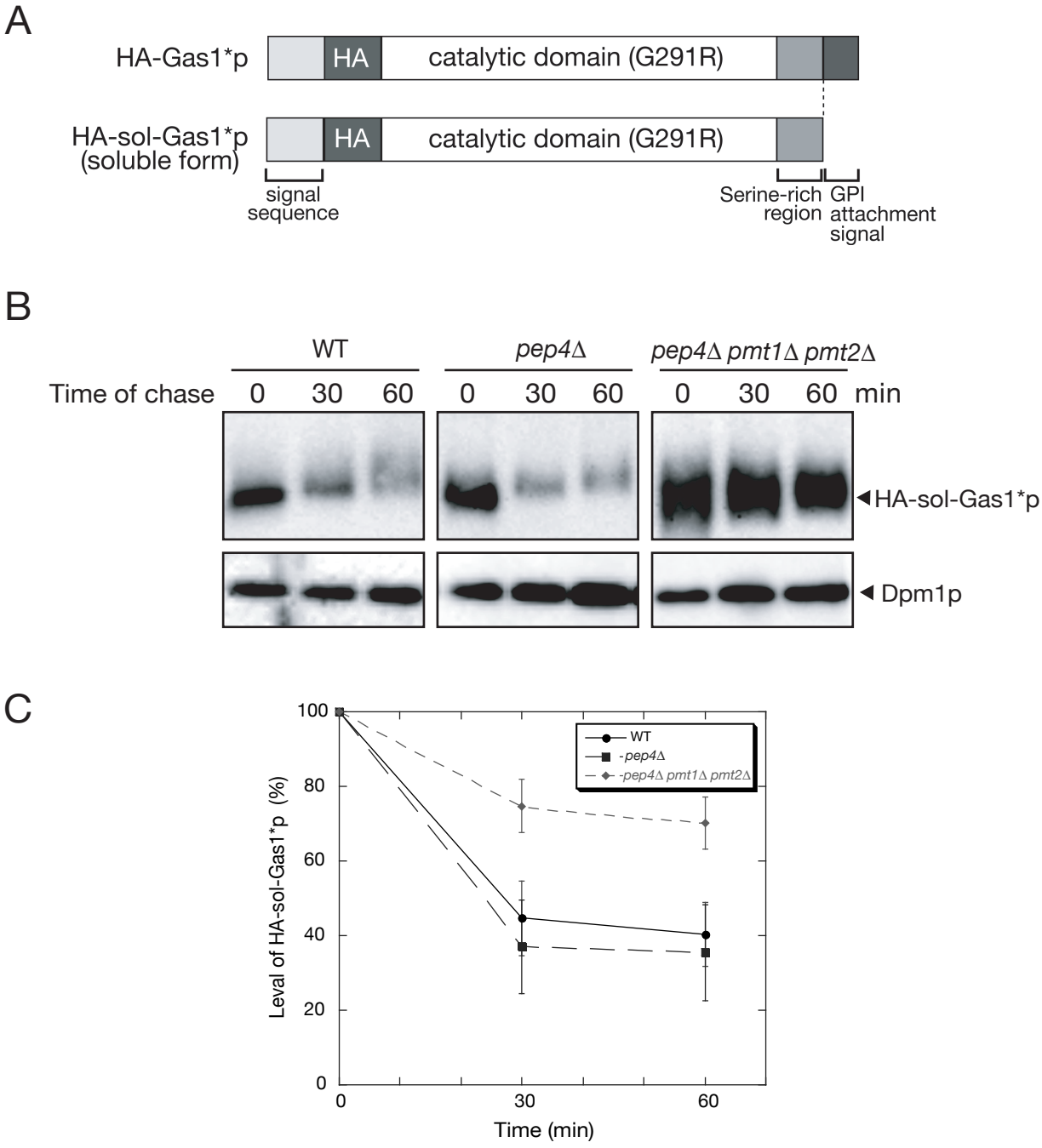

Figure 13. HA-sol-Gas1*p is also degraded in the vacuole in *pmt1*Δ *pmt2*Δ double-mutant cells

(A) Construction of HA-Gas1*p and HA-sol-Gas1*p. HA-sol-Gas1*p carry a stop codon instead of an asparagine (N538) just before the GPI anchor attatchment signal of Gas1p. (B) CHX-chase experiment in wild-type (YME1398), *pep4*Δ (YME1399), and *pep4*Δ *pmt1*Δ *pmt2*Δ (YME1400) cells expressing HA-sol-Gas1*p. Exponentially-grown cells were incubated with 200 μg/ml of CHX, and 1.0 OD_{600} units of cells were recovered at the indicated time points. Then 5 μl of each sample was separated by SDS-PAGE and analyzed by Immunoblotting with anti-HA antibody. The Immunoblot was subsequently probed with anti-Dpm1p as a control for protein loading. (C) The relative amounts of HA-sol-Gas1*p were quantified with an image analyzer and plotted as mean values ± SD from three independent experiments, with the quantity at the 0 time point set at 100%.

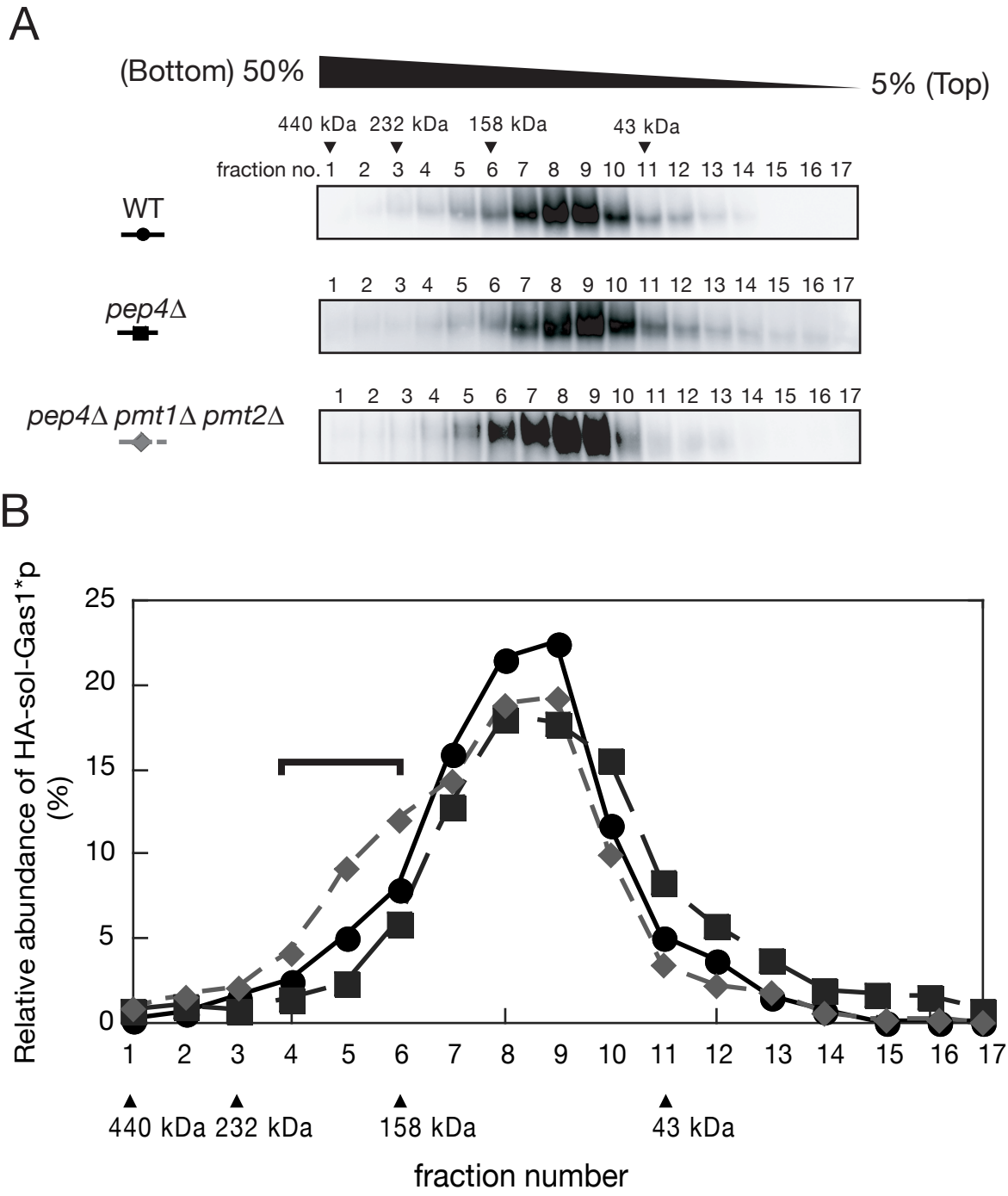

Figure 14. HA-sol-Gas1*p expressed in *pep4*Δ *pmt1*Δ *pmt2*Δ cells was more aggregated than that in wild-type and *pep4*Δ cells

(A) Whole-cell lysates were prepared from HA-sol-Gas1*p expressing wild-type (YME1398), *pep4*Δ (YME1399), and *pep4*Δ *pmt1*Δ *pmt2*Δ (YME1400) cells. Cell lysates were subjected to 5–50% linear sucrose density gradient centrifugation. Fractions were collected and analyzed by SDS-PAGE, followed by Immunoblotting using an anti-HA antibody (1:8000) and HRP-conjugated anti-mouse IgG antibody (1:8000) (see "**Materials and methods**"). (B) Relative amounts of HA-sol-Gas1*p in each fraction were quantified. Vertical arrowheads indicate the position of ferritin (440 kDa), catalase (232 kDa), aldolase (158 kDa), and ovalbumin (43 kDa).

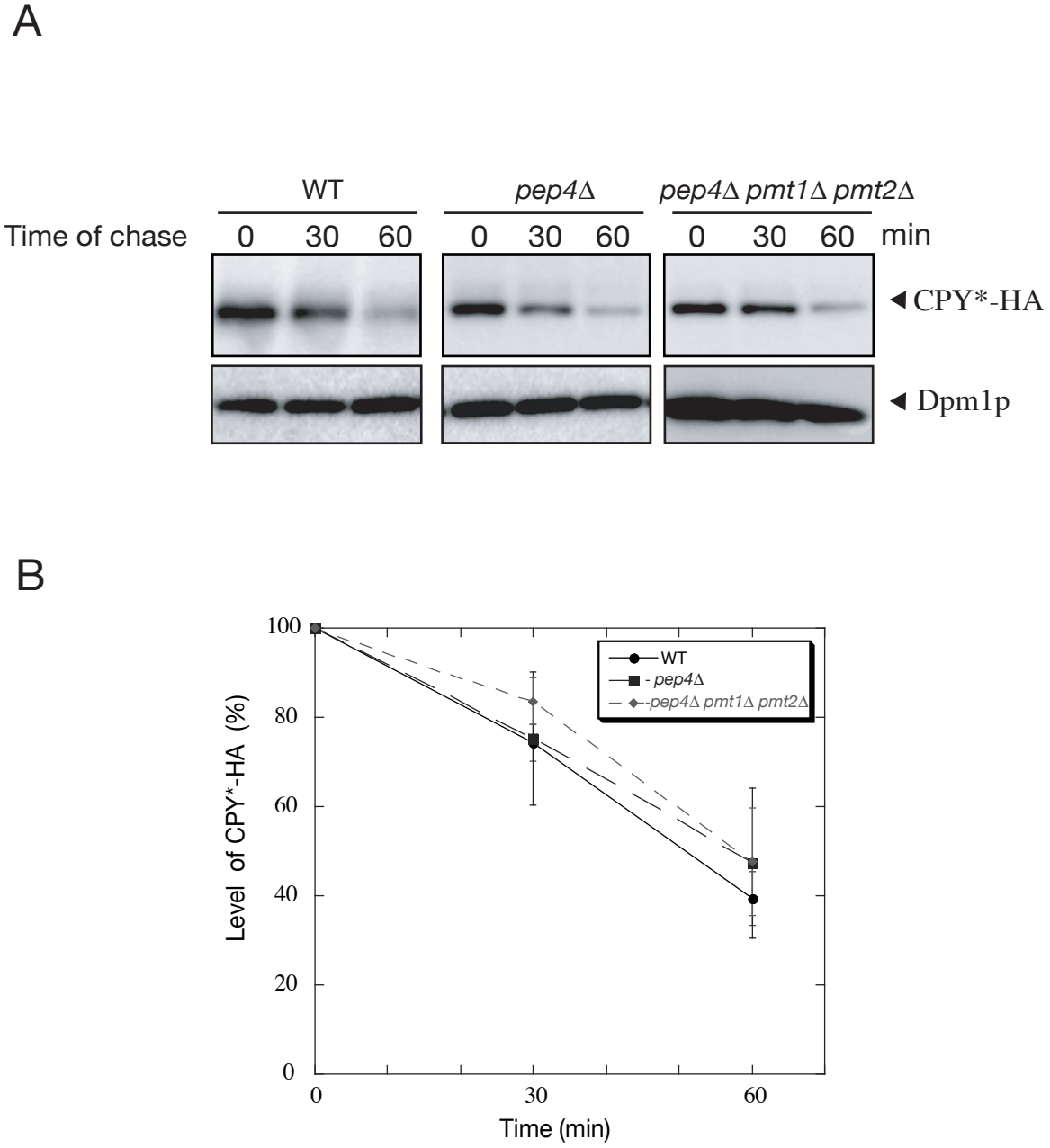

Figure 15. Deletion of *PEP4* has no effect on degradation of CPY* in *pmt1*Δ *pmt2*Δ cells.

(A) CHX-chase experiment of CPY*-HA expressed in wild-type (YME1421), *pep4*Δ (YME1422), and *pep4*Δ *pmt1*Δ *pmt2*Δ (YME1423) cells. Five OD_{600} units of cells were recovered at the indicated time points. Then 5 µl of each sample was separated by SDS-PAGE and analyzed by Immunoblotting as described in Fig. 4A. (B) The relative amounts of CPY*-HA were quantified as described in Figure 13C.

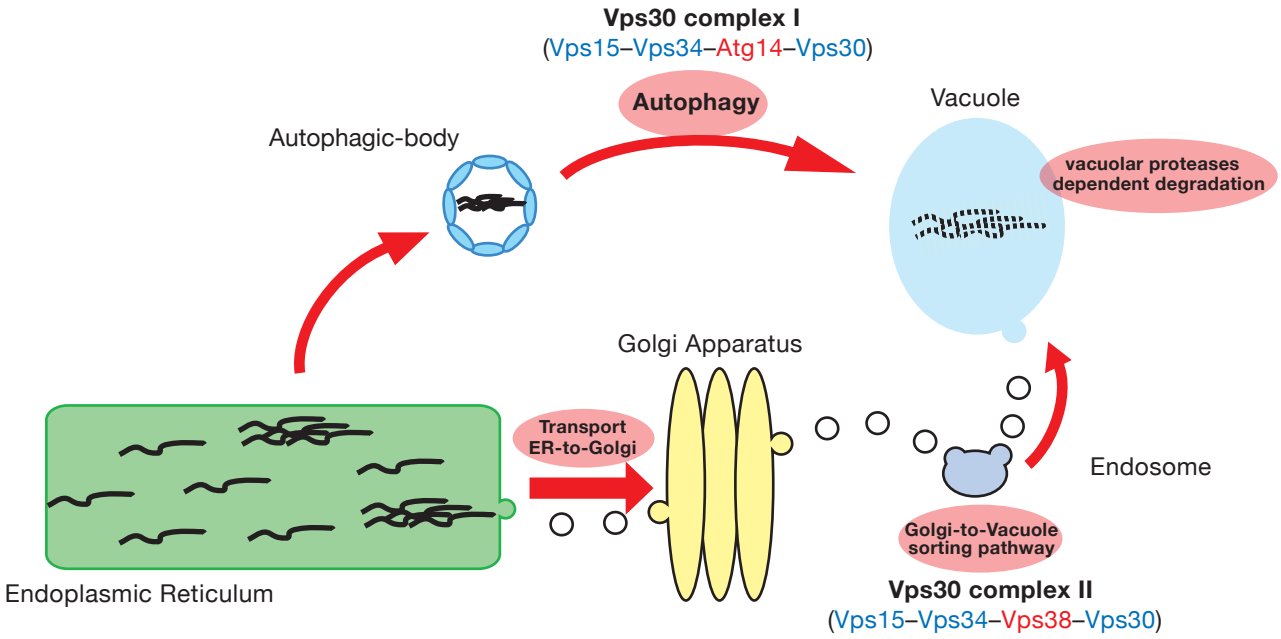

Figure 16. Two pathways transport misfolded proteins to the vacuole

In post-ER degradation, misfolded model proteins, which are degraded by vacuolar proteases, are targeted to the vacuole via two routes; the Golgi-to-vacuole sorting pathway or the autophagic pathway.

A

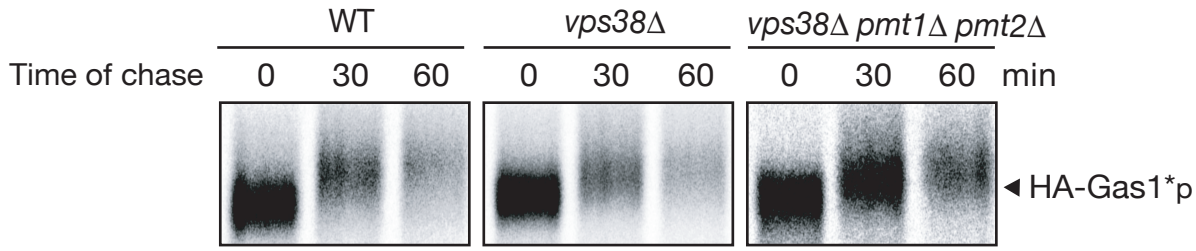

B

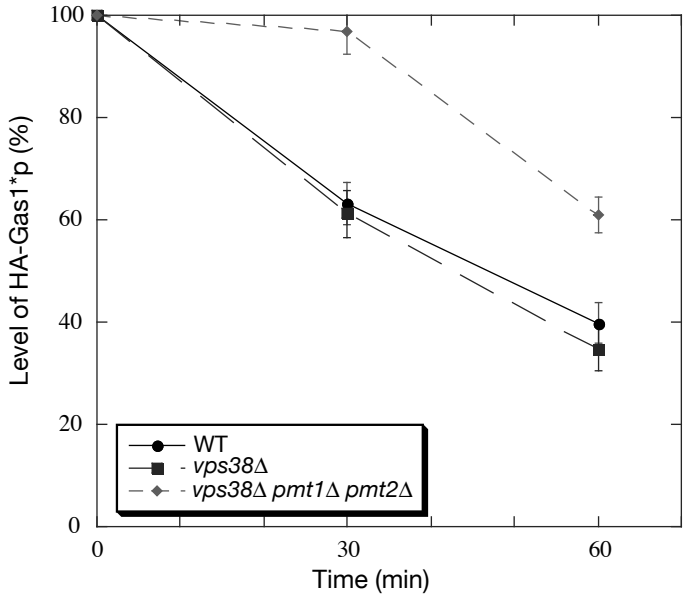

Figure 17. Degradation rate of HA-Gas1*p is reduced in *vps38*Δ *pmt1*Δ *pmt2*Δ cells

(A) HA-Gas1*p expressed in wild-type (YME1305), *vps38*Δ (YME1444), and *vps38*Δ *pmt1*Δ *pmt2*Δ (YME1440) cells were pulse-labeled with [^{35}S]-cysteine/methionine as described in Fig. 3. (B) The relative amounts of HA-Gas1*p were quantified as described in Figure 12. Error bars indicate means values ± SD from three independent experiments.

Figure 18. Model for the function of *O*-mannosylation, executed by Pmt1p and Pmt2p, to Gas1*p in ERQC systems

In wild-type cells, excessively *O*-mannosylated Gas1*p can exit the ER and target to ERAD via ERAD-L pathway and is degraded by 26S proteasome (A). on the other hand, underglycosylated Gas1*p, due to the defect of Pmt1p and Pmt2p, forms weakly aggregated oligomer and is degraded vacuole proteases dependently after sending to the vacuole via Golgi apparatus (B). Taken together, *O*-mannosylation that is executed by Pmt1p and Pmt2p to Gas1*p is not only contribute to alleviation of aggregation of Gas1*p but also may be function as a 'slection tag' in ERQC/ERAD mechanism.

A Degradation of Gas1*p (wild-type cell)

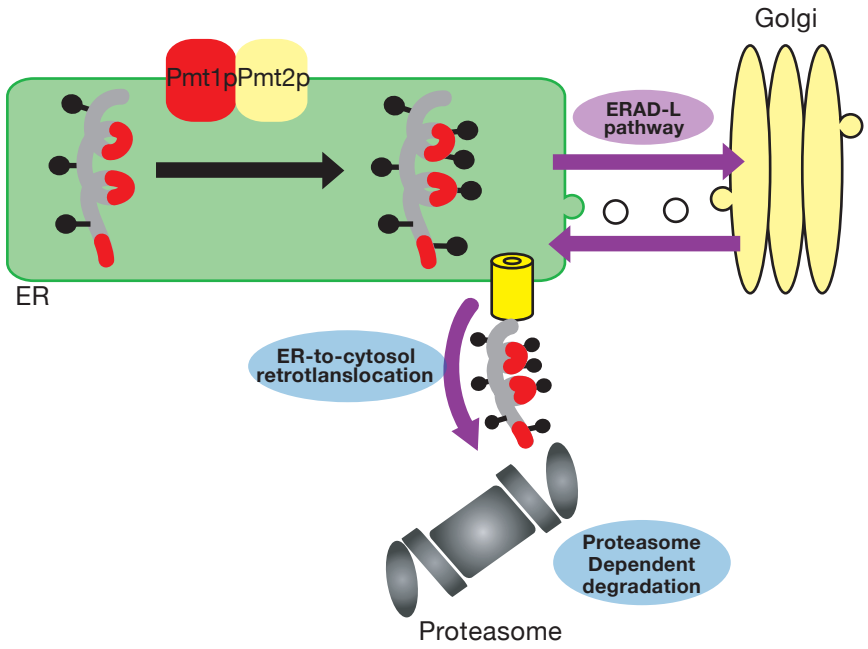

B Degradation of Gas1*p (*pmt1*Δ *pmt2*Δ cell)